directly, and promoted meniscal regeneration without mobilization to distant organs.

Acknowledgments

We thank Miyoko Ojima for expert help with histology, Yasuko Sakuma for help with animal experiments, and Noriko Hashimoto for skillful technical assistance with microarray and real-time PCR analyses. This study was supported by grants from "the Japan Society for the Promotion of Science (16591478)" to I.S. and "the Japanese Ministry of Education Global Center of Excellence (GCOE) Program, International Research Center for Molecular Science in Tooth and Bone Diseases" to T.M.

Disclosure of Potential Conflicts of Interest

The authors indicate no potential conflicts of interest.

References

1 Wieland HA, Michaelis M, Kirschbaum BJ et al. Osteoarthritis—An untreatable disease? Nat Rev Drug Discov 2005;4:331–344.
2 Chen FH, Rousche KT, Tuan RS. Technology insight: Adult stem cells in cartilage regeneration and tissue engineering. Nat Clin Pract Rheumatol 2006;2:373–382.
3 Ratajczak W. Early development of the cruciate ligaments in staged human embryos. Folia Morphol (Warsz) 2000;59:285–290.
4 Sakaguchi Y, Sekiya I, Yagishita K et al. Comparison of human stem cells derived from various mesenchymal tissues: Superiority of synovium as a cell source. Arthritis Rheum 2005;52:2521–2529.
5 Yoshimura H, Muneta T, Nimura A et al. Comparison of rat mesenchymal stem cells derived from bone marrow, synovium, periosteum, adipose tissue, and muscle. Cell Tissue Res 2007;327:449–462.
6 Morito T, Muneta T, Hara K et al. Synovial fluid-derived mesenchymal stem cells increase after intra-articular ligament injury in humans. Rheumatology (Oxford) 2008;47:1137–1143.
7 Zhang S, Muneta T, Morito T et al. Autologous synovial fluid enhances migration of mesenchymal stem cells from synovium of osteoarthritis patients in tissue culture system. J Orthop Res 2008;26: 1413–1418.
8 Hakamata Y, Murakami T, Kobayashi E. "Firefly rats" as an organ/cellular source for long-term in vivo bioluminescent imaging. Transplantation 2006;81:1179–1184.
9 Inoue H, Ohsawa I, Murakami T et al. Development of new inbred transgenic strains of rats with LacZ or GFP. Biochem Biophys Res Commun 2005;329:288–295.
10 Sekiya I, Larson BL, Vuoristo JT et al. Adipogenic differentiation of human adult stem cells from bone marrow stroma (MSCs). J Bone Miner Res 2004;19:256–264.
11 Sekiya I, Vuoristo JT, Larson BL et al. In vitro cartilage formation by human adult stem cells from bone marrow stroma defines the sequence of cellular and molecular events during chondrogenesis. Proc Natl Acad Sci USA 2002;99:4397–4402.
12 Kato A, Homma T, Batchelor J et al. Interferon-α/β receptor-mediated selective induction of a gene cluster by CpG oligodeoxynucleotide 2006. BMC Immunol 2003;4:8.
13 Quackenbush J. Computational analysis of microarray data. Nat Rev Genet 2001;2:418–427.
14 Contag PR, Olomu IN, Stevenson DK et al. Bioluminescent indicators in living mammals. Nat Med 1998;4:245–247.
15 Ichinose S, Tagami M, Muneta T et al. Morphological examination during in vitro cartilage formation by human mesenchymal stem cells. Cell Tissue Res 2005;322:217–226.
16 Murphy JM, Fink DJ, Hunziker EB et al. Stem cell therapy in a caprine model of osteoarthritis. Arthritis Rheum 2003;48:3464–3474.
17 Caplan AI, Dennis JE. Mesenchymal stem cells as trophic mediators. J Cell Biochem 2006;98:1076–1084.
18 Abdel-Hamid M, Hussein MR, Ahmad AF et al. Enhancement of the repair of meniscal wounds in the red-white zone (middle third) by the injection of bone marrow cells in canine animal model. Int J Exp Pathol 2005;86:117–123.
19 Agung M, Ochi M, Yanada S et al. Mobilization of bone marrow-derived mesenchymal stem cells into the injured tissues after intra-articular injection and their contribution to tissue regeneration. Knee Surg Sports Traumatol Arthrosc 2006;14:1307–1314.
20 Ochi M, Uchio Y, Okuda K et al. Expression of cytokines after meniscal rasping to promote meniscal healing. Arthroscopy 2001;17: 724–731.
21 Nimura A, Muneta T, Koga H et al. Increased proliferation of human synovial mesenchymal stem cells with autologous human serum: comparisons with bone marrow mesenchymal stem cells and with fetal bovine serum. Arthritis Rheum 2008;58:501–510.
22 Wakitani S, Takaoka K, Hattori T et al. Embryonic stem cells injected into the mouse knee joint form teratomas and subsequently destroy the joint. Rheumatology (Oxford) 2003;42:162–165.
23 Takahashi K, Yamanaka S. Induction of pluripotent stem cells from mouse embryonic and adult fibroblast cultures by defined factors. Cell 2006;126:663–676.
24 Koga H, Shimaya M, Muneta T et al. Local adherent technique for transplanting mesenchymal stem cells as a potential treatment of cartilage defect. Arthritis Res Ther 2008;10:R84.
25 Koga H, Muneta T, Ju YJ et al. Synovial stem cells are regionally specified according to local microenvironments after implantation for cartilage regeneration. Stem Cells 2007;25:689–696.
26 Segawa Y, Muneta T, Makino H et al. Mesenchymal stem cells derived from synovium, meniscus, anterior cruciate ligament, and articular chondrocytes share similar gene expression profiles. J Orthop Res 2008 [Epub ahead of print].
27 Koga H, Muneta T, Nagase T et al. Comparison of mesenchymal tissues-derived stem cells for in vivo chondrogenesis: Suitable conditions for cell therapy of cartilage defects in rabbit. Cell Tissue Res 2008; 333:207–215.
28 Mizuno K, Muneta T, Morito T et al. Exogenous synovial stem cells adhere to defect of meniscus and differentiate into cartilage cells. J Med Dent Sci 2008;55:101–111.
29 Cannon WD Jr., Vittori JM. The incidence of healing in arthroscopic meniscal repairs in anterior cruciate ligament-reconstructed knees versus stable knees. Am J Sports Med 1992;20:176–181.
30 Arnoczky SP, Warren RF. The microvasculature of the meniscus and its response to injury. An experimental study in the dog. Am J Sports Med 1983;11:131–141.
31 Bendjaballah MZ, Shirazi-Adl A, Zukor DJ. Biomechanics of the human knee joint in compression: Reconstruction, mesh generation and finite element analysis. Knee 1995;2:69–79.
32 Gabrion A, Aimedieu P, Laya Z et al. Relationship between ultrastructure and biomechanical properties of the knee meniscus. Surg Radiol Anat 2005;27:507–510.
33 McDevitt CA, Webber RJ. The ultrastructure and biochemistry of meniscal cartilage. Clin Orthop Relat Res 1990;8–18.
34 McGonagle D, Jones E. A potential role for synovial fluid mesenchymal stem cells in ligament regeneration. Rheumatology (Oxford) 2008;47:1114–1116.
35 Iso Y, Spees JL, Serrano C et al. Multipotent human stromal cells improve cardiac function after myocardial infarction in mice without long-term engraftment. Biochem Biophys Res Commun 2007;354: 700–706.
36 Lee RH, Seo MJ, Pulin AA et al. The CD34-like protein PODXL and {alpha}6-integrin (CD49f) identify early progenitor MSCs with increased clonogenicity and migration to infarcted heart in mice. Blood 2009;113:816–826.

Biochemical and Biophysical Research Communications 378 (2009) 600–604

Contents lists available at ScienceDirect

Biochemical and Biophysical Research Communications

journal homepage: www.elsevier.com/locate/ybbrc

Latexin is involved in bone morphogenetic protein-2-induced chondrocyte differentiation

Ichiro Kadouchi [a,b], Kei Sakamoto [b], Liu Tangjiao [b,c], Takashi Murakami [d], Eiji Kobayashi [d], Yuichi Hoshino [a], Akira Yamaguchi [b,e,*]

[a] Department of Orthopedic Surgery, Jichi Medical University, Shimotsuke, Tochigi, Japan
[b] Section of Oral Pathology, Department of Oral Restitution, Graduate School of Tokyo Medical and Dental University, Bunkyo-ku, Tokyo 113-8549, Japan
[c] Section of Oral Pathology, College of Stomatology, Dalian Medical University, Dalian, China
[d] Division of Organ Replacement Research, Center for Molecular Medicine, Jichi Medical University, Shimotsuke, Tochigi, Japan
[e] Global Center of Excellence Program, International Research Center for Molecular Science in Tooth and Bone Diseases, Graduate School of Tokyo Medical and Dental University, Bunkyo-ku, Tokyo 113-8549, Japan

ARTICLE INFO

Article history:
Received 17 November 2008
Available online 4 December 2008

Keywords:
Latexin
BMP-2
Chondrocyte
Bone regeneration
Cartilage
Bone fracture

ABSTRACT

Latexin is the only known carboxypeptidase A inhibitor in mammals. We previously demonstrated that BMP-2 significantly induced *latexin* expression in Runx2-deficient mesenchymal cells (RD-C6 cells), during chondrocyte and osteoblast differentiation. In this study, we investigated latexin expression in the skeleton and its role in chondrocyte differentiation. Immunohistochemical studies revealed that proliferating and prehypertrophic chondrocytes expressed latexin during skeletogenesis and bone fracture repair. In the early phase of bone fracture, *latexin* mRNA expression was dramatically upregulated. BMP-2 upregulated the expression of the mRNAs of *latexin*, *Col2a1*, and the gene encoding aggrecan (*Agc1*) in a micromass culture of C3H10T1/2 cells. Overexpression of *latexin* additively stimulated the BMP-2-induced expression of the mRNAs of *Col2a*, *Agc1*, and *Col10a1*. BMP-2 treatment upregulated *Sox9* expression, and *Sox9* stimulated the promoter activity of *latexin*. These results indicate that latexin is involved in BMP-2-induced chondrocyte differentiation and plays an important role in skeletogenesis and skeletal regeneration.

Chondrocytes and osteoblasts originate from common progenitors called mesenchymal stem cells [1]. During the differentiation of these cells, bone morphogenetic proteins (BMPs) play a crucial role in inducing the expression of lineage-specific transcription factors such as Runx2 [1–3] and Sox9 [4,5]; Runx2 is an essential transcription factor that regulates osteoblast differentiation [1,6,7] and chondrocyte maturation [8], and Sox9 is an important transcription factor that regulates chondrocyte differentiation from mesenchymal stem cells [5,9].

We established a clonal cell line, RD-C6, from *Runx2*-deficient mouse embryos and demonstrated that this cell line could differentiate into both osteoblasts and chondrocytes in response to BMP-2 treatment via a Runx2-independent pathway [10]. By microarray analysis of this cell line with and without BMP-2 treatment, we identified latexin as a downstream factor of BMP-2 signaling [10]. This implied that latexin expression was regulated by BMP-2 signaling via a Runx2-independent pathway.

Latexin is composed of 222 amino acids and has a molecular weight of 29 kDa; further, it is the only known carboxypeptidase A inhibitor in mammals [11,12]. The latexin was discovered in the lateral neocortex of rats, and it acts as a marker of regionality and development of both the central and the peripheral nervous systems [11]. Further, *latexin* is expressed in several other tissues, including hematopoietic and lymphoid organs, and plays an important role in regulating the activity of hematopoietic stem cells [12,13]. By microarray analysis, Balint et al. [14] briefly mentioned that *latexin* was one of the upregulated genes in BMP-2-treated C2C12 cells. This suggests a possible role of latexin in osteoblast differentiation, because C2C12 cells exclusively differentiated into osteoblasts and not into chondrocytes by BMP-2 treatment [15]. In addition, we demonstrated that BMP-2 induced RD-C6 cells to differentiate into both osteoblast and chondrocyte lineage cells [10]. However, it remained unclear whether latexin is involved in osteogenic differentiation, chondrogenic differentiation, or both.

To investigate the role of latexin in skeletal cell differentiation, we first investigated latexin expression during skeletogenesis and skeletal regeneration and examined its role in chondrocyte differentiation by using a multipotent mesenchymal cell line, C3H10T1/2. Here, we describe that latexin is expressed in chondrocytes and involved in BMP-2-induced chondrocyte differentiation.

* Corresponding author. Address: Section of Oral Pathology, Department of Oral Restitution, Graduate School of Tokyo Medical and Dental University, Bunkyo-ku, Tokyo 113-8549, Japan. Fax: +81 3 5803 0188.
E-mail address: akira.mpa@tmd.ac.jp (A. Yamaguchi).

0006-291X/$ - see front matter © 2008 Elsevier Inc. All rights reserved.
doi:10.1016/j.bbrc.2008.11.111

Materials and methods

Immunohistochemistry. Immunohistochemical staining was performed on 4% paraformaldehyde-fixed, ethylenediaminetetraacetic acid (EDTA)-decalcified, and paraffin-embedded sections. Endogenous peroxidase activity was blocked with 10% hydrogen peroxidase/methanol, and nonspecific binding was blocked with 10% horse serum. The sections were incubated with goat anti-latexin (Everest Biotech, Oxfordshire, UK) or rabbit anti-Sox9 (Santa Cruz Biotechnology Inc., Santa Cruz, CA) overnight at 4 °C. After washing, they were incubated with horseradish peroxidase-conjugated secondary antibodies (Dako, Glostrup, Denmark). The antigen-bound peroxidase activity was visualized by staining the sections with 3-amino-9-ethyl-carbazole (AEC) chromogen.

Fracture model. The midshafts of the tibiae of 8-week-old mice were fractured using a bone saw and internally stabilized with an intramedullary nail by using the inner pin of a spinal needle with 22-G diameter. The mice were sacrificed and submitted for histological and real-time reverse-transcriptase polymerase chain reaction (RT-PCR) analyses on 5, 10, and 15 days after the operation. All animal studies were approved by the Animal Ethics Committee of Jichi Medical University and performed in accordance with the Jichi Medical University Guide for the Care and Use of Laboratory Animals, following the principles of laboratory animal care formulated by the National Society for Medical Research.

Cell culture. C3H10T1/2 (clone 8) cells were purchased from Cell Bank, RIKEN BioResource Center (Tsukuba, Japan). The cells were maintained in Eagle's basal medium containing 10% fetal bovine serum (FBS; Sigma, St. Louis, MO), L-glutamine, 50 U/ml penicillin G, and 50 mg/ml streptomycin. For a micromass culture, the C3H10T1/2 cells were suspended in the medium at a concentration of 1×10^7 cells/ml, and a 10-μl drop of this cell suspension was placed in the center of a culture dish. The cells were allowed to adhere for 3 h, and a medium with or without recombinant human BMP-2 (rhBMP-2; 100 ng/ml; Astellas Pharma Inc., Tokyo, Japan) was added to the culture. The cells were stained with Alcian blue solution (pH 2.5) on days 2 and 4 *in vitro*.

Mouse cDNA containing *latexin* open reading frame was obtained by PCR and subcloned into pMSCV (Clontech, CA). Retrovirus was produced and cells were infected with the retrovirus according to the manufacturer's instructions. After infection, the cells were selected in a puromycin-containing medium for 2 weeks.

Western blot analysis. The cells were lysed with radioimmunoprecipitation assay (RIPA) buffer containing protease inhibitor cocktail (Roche Diagnostics, Basel, Switzerland). Western blot analysis was performed according to the standard procedure. SDS–polyacrylamide gel electrophoresis (PAGE) was performed using 1× sample buffer containing 5% β-mercaptoethanol. The proteins were transferred to nitrocellulose membranes, which were then incubated with the following primary antibodies for 1 h: goat anti-latexin, rabbit anti-Sox9, and anti-actin (SC-1616; Santa Cruz Biotechnology Inc.). Next, the membranes were incubated with the respective secondary antibodies for 1 h. Chemiluminescence was detected with an enhanced chemiluminescence (ECL) Plus chemiluminescence detection kit (GE Healthcare, UK).

Real-time RT-PCR. Total RNA was extracted from the cultured cells using RNA Smart Total RNA Isolation Kit (Macherey-Nagel GmbH & Co. KG, Düren, Germany). RNA aliquots of 500 ng were reverse transcribed to cDNA by using a First-Strand cDNA synthesis kit for RT-PCR (Invitrogen Corp., Carlsbad, CA) and an oligo-dT primer. mRNA expression was quantified by real-time RT-PCR, using a MiniOpticon system (Bio-Rad Laboratories, Hercules, CA) with the iQ SYBR Green supermix (Bio-Rad Laboratories). Relative amount of each mRNA was normalized to 18 S rRNA expression. The primer sequences are listed in Table 1.

Table 1
Primers used for real-time-based RT-PCR.

	Forward primer	Reverse primer
Lxn	5′- GTCGCCTGCGGTTATGTAAT	5′- GGCGGCTGTTGTGTTTTACT
Col2a1	5′-TGCACGAAACACACTGGTAAG	5′- CACCAAATTCCTGTTCAGCC
Agc1	5′- AGGAGACCCAGACAGCAGAA	5′-ACAGTGACCCTGGAACTTGG
Col10a1	5′-TGGGTAGGCCTGTATAAAGAACGG	5′-CATGGGAGCCACTAGGAATCC TGAGA
Sox9	5′- CTCGCAATACGACTACGCT	5′-CTGGTTGTTCCCAGTGCT
18S rRNA	5′-GTAACCCGTTGAACCCCATT	5′-CCATCCAATCGGTAGTAGCG

Luciferase activity assay. The proximal promoter region of human *latexin* was obtained from a bacterial artificial chromosome (BAC) clone, RP11-bA39F4, by PCR, and the product was cloned into pGL3-basic (latexin-luc; Promega, Madison, WI). The latexin-luc plasmid was transfected into C3H10T1/2 cells, using Lipofectamine 2000 (Invitrogen) according to the manufacturer's instructions. The amount of latexin-luc plasmid was 0.5 μg in every experiment. Luciferase activity was measured 48 hours after the transfection by using a luciferase assay kit (Promega) according to the manufacturer's instructions.

Statistics. Statistical analyses were performed using Student's unpaired *t*-test. Each experiment was conducted at least twice. The data presented represent means ± standard deviation (SD) of independent replicates ($n > 3$).

Results

Some chondrocytes express latexin in embryonic skeleton and regenerative bone

We first investigated latexin expression during skeletogenesis in embryonic mice and skeletal regeneration in adult mice by immunohistochemistry. Latexin expression was observed in resting to prehypertrophic chondrocytes but not in hypertrophic chondrocytes in E15.5 embryos (Fig. 1A and B). The distribution of latexin-positive cells was similar to that of Sox9-positive cells (Fig. 1C and D). Some osteoblastic cells at periosteoal region in bone collar showed weak signals for latexin expression (Fig. 1A). The peripheral nerves at perichondral membrane exhibited strong signals of latexin (Fig. 1A).

We next examined latexin expression during bone fracture healing at the tibial diaphyses by immunohistochemistry (Fig. 1E–J). In our experimental model, chondrocytes appeared at the periosteal region around the bone fracture site on day 5 after the injury (Fig. 1E). Immunohistochemical studies revealed that many of these chondrocytes were positive for latexin (Fig. 1F). Interestingly, immunoreactivity was detected in the nuclei as well as the cytoplasm of numerous chondrocytes. Numerous hypertrophic chondrocytes and newly formed trabecular bones were observed on day 10, but only proliferating or prehypertrophic chondrocytes were positive for latexin (Fig. 1G and H). Hypertrophic chondrocytes showed no apparent signals for latexin expression (Fig. 1H). On day 15, the process of new bone formation progressed by replacing the preexisting cartilage (Fig. 1I), and osteoblasts covering newly formed bone trabeculae showed no apparent signals of latexin (Fig. 1J). The number of latexin-positive cells dramatically decreased on day 15 as compared with those on days 5 and 10. No apparent signals were found in the osteoblastic cells covering the trabecular and cortical bones away from fracture sites.

Real-time RT-PCR analysis confirmed that *latexin* expression was undetectable before the injury; however, its expression dramatically increased on day 5 after the injury and then gradually declined on days 10 and 15 (Fig. 1K).

These results indicate that latexin is expressed in chondrogenic cells during skeletogenesis in mouse embryos, and its expression is

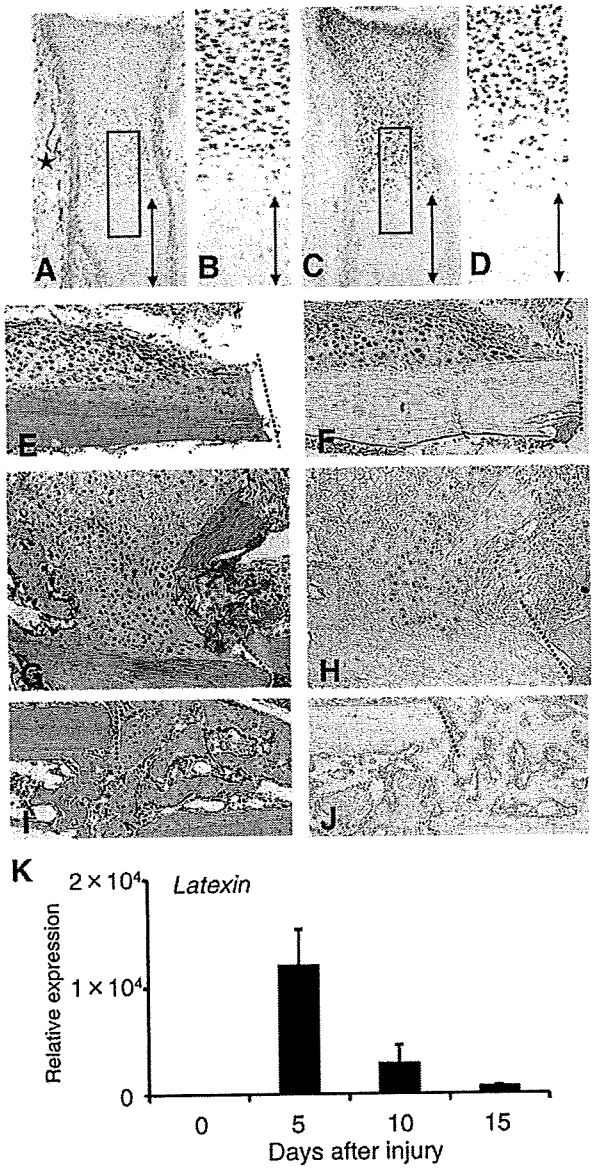

Fig. 1. Chondrocytes express latexin expression in the embryonic tibiae (A,B) and during skeletal regeneration in adult mice (F, H, and J). (A,B) Immunohistochemical staining of latexin in the tibia of an E15.5 mouse embryo. A higher magnification image of the square in A is shown in B. (C,D) Immunohistochemical staining of Sox9 in the tibia of an E15.5 mouse embryo. A higher magnification image of the square in C is shown in D. Arrows in A, B, C, and D indicate hypertrophic chondrocytes zones. An asterisk in A shows latexin-positive peripheral nerves. (E, G, and I) Hematoxylin–eosin staining images of fracture repair on days 5 (E), 10 (G) and 15 (I) after injury in tibiae of adult mice. (F, H, and J) Immunohistochemical staining of latexin during fracture repair. Note that latexin-positive chondrocytes in F and H. Hypertrophic chondrocytes in H and osteoblasts covering newly formed bone trabeculae exhibit few signals for latexin. Dotted lines in E–J indicate fracture end of cortical bones. (K) *Latexin* mRNA expression during fracture repair assessed by real-time RT-PCR as described in Materials and methods.

limited to the chondrocytes appearing during fracture repair in adult mice.

BMP-2 induces latexin expression in C3H10T1/2 cells along with chondrocyte differentiation

To investigate the role of latexin in chondrocyte differentiation, we used a micromass culture of C3H10T1/2 cells. The cultured cells produced Alcian blue-positive extracellular matrix on day 2, the amount of which increased on day 4 in the culture (Fig. 2A). BMP-2 treatment increased the production of Alcian blue-positive extracellular matrix on days 2 and 4 as compared with the respective control cultures (Fig. 2A). The treatment significantly increased the *in vitro* expression of the mRNA for *Col2a1* and *aggrecan* (*Agc1*), which encode the major components of extracellular matrices synthesized by chondrocytes, on days 2 and 4 (Fig. 2B). These results indicate that C3H10T1/2 cells maintained in a micromass culture differentiate into chondrogenic cells in response to BMP-2. We next investigated *latexin* expression in C3H10T1/2 cells cultured in this system by real-time RT-PCR and Western blot analysis. BMP-2 upregulated the latexin expression on days 2 and 4 at the mRNA and protein levels (Fig. 2C and D). These results suggest that BMP-2 induces latexin expression along with chondrocyte differentiation.

Overexpression of latexin stimulates BMP-2-induced chondrocyte differentiation

We overexpressed mouse *latexin* gene in C3H10T1/2 cells by infecting the cells with a retrovirus. The infected cells were cultured with and without rhBMP-2 for 2 days. The cells overexpressing *latexin* induced no changes in the expression of the mRNAs of *Col2a1*, *Agc1*, and *Col10a1* in the absence of BMP-2, compared with the control culture (Fig. 3). In contrast, the cells overexpressing *latexin* significantly increased the expression of the abovementioned mRNAs in the presence of BMP-2, as compared with the BMP-2-treated cells transduced with green fluorescent protein (GFP) (Fig. 3). These results suggest that latexin additively stimulates BMP-2-induced chondrocyte differentiation.

Sox9 stimulates the promoter activity of latexin

BMP-2 induced *latexin* expression in RD-C6 cells, Runx2-deficient cell line, as well as in C3H10T1/2 cells. These results prompted us to investigate whether BMP-2 directly stimulated the promoter activity of *latexin*, and we found that BMP-2 treatment induced no apparent stimulation of the promoter activity of *latexin* at concentrations of 100 and 500 ng/ml (data not shown). It has been reported that BMP-2 efficiently induces *Sox9* expression along with chondrogenic differentiation [4,5], and we also confirmed BMP-2-induced upregulation of *Sox9* mRNA expression in C3H10T1/2 cells on day 2 (Fig. 4A). Therefore, we investigated whether *Sox9* regulates the promoter activity of *latexin*. As shown in Fig. 4B, Sox9 stimulated the promoter activity of *latexin*. These findings suggest that BMP-2-induced Sox9 regulates *latexin* expression in chondrogenic differentiation.

Discussion

Latexin is expressed in various tissues, including brain tissues and hematopoietic and lymphoid organs [11–13,16,17], but its expression and function in skeletal tissues have not been reported in detail. We previously identified *latexin* as a downstream factor of BMP signaling by a microarray analysis of RD-C6 cells, a Runx2-deficient cell line, with and without BMP-2 treatment [10]. Since BMP-2 treatment induced RD-C6 cells to differentiate into both osteoblasts and chondrocytes [10], we first investigated latexin expression during skeletogenesis and skeletal regeneration to identify the skeletal cells that express latexin *in vivo* by immunohistochemistry. This study revealed that the proliferating and pre-hypertrophic chondrocytes in the embryonic tibiae and callus appearing during skeletal regeneration in adult mice expressed latexin. Real-time RT-PCR analysis also indicated the great induction

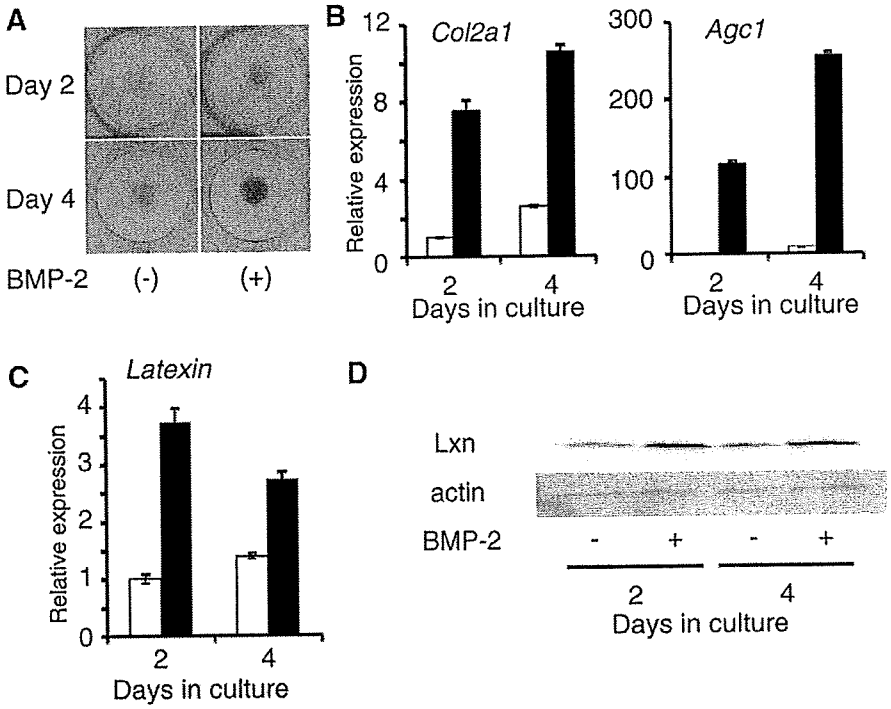

Fig. 2. BMP-2 stimulated the expression of *latexin* mRNA in a micromass culture of C3H10T1/2 cells along with chondrocyte differentiation. (A) Alcian blue staining of C3H10T1/2 cells cultured with and without BMP-2 (100 ng/ml) for 2 and 4 days. (B) Effects of BMP-2 on mRNA expression for *Col2a1* and *Agc1*. C3H10T1/2 cells were cultured for 2 and 4 days in the absence (open bars) and presence (closed bars) of BMP-2, and the expression of the abovementioned mRNAs was determined by real-time RT-PCR. (C) Effects of BMP-2 on the expression of *latexin* mRNA. C3H10T1/2 cells were cultured for 2 and 4 days in the absence (open bars) and presence (closed bars) of BMP-2. (D) Effects of BMP-2 on latexin expression. C3H10T1/2 cells were cultured for 2 and 4 days in the absence and presence of BMP-2, and latexin expression was examined by Western blot analysis as described in Materials and methods.

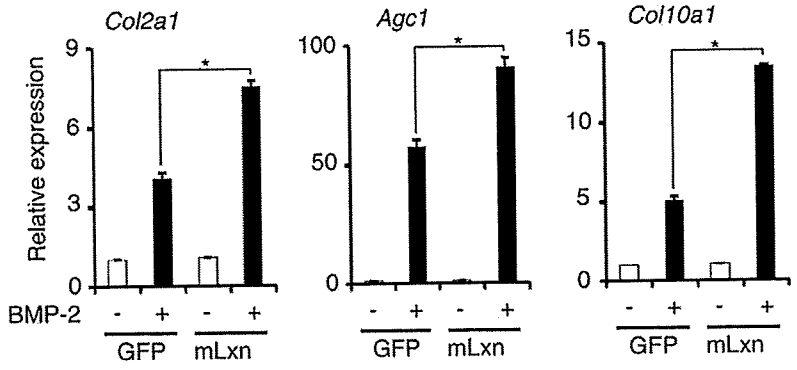

Fig. 3. Overexpression of latexin stimulated BMP-2-induced chondrocyte differentiation in a micromass culture of C3H10T1/2 cells. The cells were cultured for 2 days with and without BMP-2 (100 ng/ml). The expression of the mRNAs of *Col2a*, *Agc1*, and *Col10a1* were determined by real-time RT-PCR as described in Materials and methods). Relative amount of each mRNA was normalized to 18S rRNA expression. $^{*}P < 0.05$ versus control cells.

of *latexin* mRNA expression in the early phase of skeletal regeneration. Taken together, these results suggest that latexin plays an important role in skeletogenesis and skeletal regeneration.

These immunohistochemical findings prompted us to investigate the role of latexin in chondrocyte differentiation, for which we used a micromass culture of C3H10T1/2 cells. The culture experiments revealed that the expression of *latexin* mRNA correlated with that of other chondrocyte differentiation-related mRNAs such as those of *Col2a1* and *Agc1*. In addition, overexpression of *latexin* additively stimulated BMP-2-induced chondrocyte differentiation. Interestingly, overexpression of latexin induced no significant changes in the expression of the abovementioned mRNAs in the absence of BMP-2, suggesting a close interaction between the regulation of *latexin* expression and BMP signaling. To further investigate the underlying mechanism, we examined the effects of BMP-2 on the activation of *latexin* promoter and found that BMP-2 did not stimulate the promoter. Since it has been reported that BMP-2 induces Sox9 expression [4,5], we examined the effects of *Sox9* on the transactivation of *latexin* promoter and demonstrated that *Sox9* stimulated the promoter activity of *latexin*. These results suggest that latexin is involved in chondrocyte differentiation via Sox9, the expression of which is upregulated by BMP-2. There have been no reports about the regulatory mechanism of *latexin* expression even in neural tissues, and *Sox9* is the first candidate transcription factor that regulates *latexin* expression. However, its *latexin*-transducing activity was not observed to be

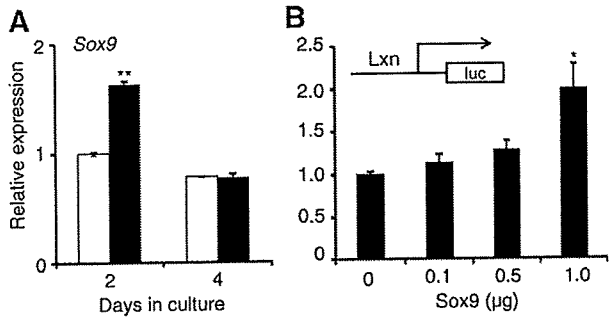

Fig. 4. BMP-2 induced the expression of *Sox9* mRNA in C3H10T1/2 cells, and Sox9 activated the promoter activity of *latexin*. (A) Effects of BMP-2 on the expression of *Sox9* mRNA in C3H10T1/2 cells on day 2, determined by real-time RT-PCR analysis. $^{**}P < 0.0001$ versus control cells. (B) Effect of Sox9 on the promoter activity of *latexin*. Data represent the fold inductions relative to the induction by mock vector transfection. $^{*}P < 0.05$ versus control cells.

strong. These findings suggest that activation of *latexin* transcription requires other transcription factors or coactivators of Sox9 such as Sox5, Sox6, and cAMP response element binding (CREB)-binding protein (CBP)/p300 [18–21].

Latexin is the only known endogenous carboxypeptidase A inhibitor in mammals [12]. It is structurally composed of two nearly identical domains that have a high conformational homology with the cystatins [22]. *Latexin* has the potential heparin/heparan sulfate-binding sites and directly interacts with a heparin component in a mast cell culture [22,16]. Heparan sulfate is an important component of the extracellular matrix of cartilage and essential for chondrocyte differentiation [23,24]. This suggests an interaction between latexin and heparan sulfate during extracellular matrix synthesis in cartilage. Our immunohistochemical study revealed the nuclear localization of latexin in chondrocytes appearing during fracture repair. It will be interesting to investigate the interaction between latexin and heparan sulfate in the nuclei, because some reports have indicated the nuclear localization of heparin sulfate [25].

In the present study, we demonstrated that latexin is expressed in chondrocytes during skeletogenesis and skeletal regeneration. *Latexin*-deficient mice, which were provided by Dr. Arimitsu [26], exhibited no growth retardation or apparent radiographic changes in the skeleton (unpublished results), suggesting the limited changes in the skeletal tissues of the mice. Since the present study revealed the dramatic upregulation of *latexin* mRNA expression in the early phase of fracture repair, it will be interesting to investigate the process of fracture repair in *latexin*-deficient mice. Such studies are currently being conducted by our group. The findings of these studies will provide important information regarding the role of latexin in skeletal growth and regeneration.

Acknowledgments

This work was supported by the Research Award to Jichii Medical University Graduate Student (I.K.) and a Grant-in-Aid for Scientific Research from the Japan Society for the Promotion of Science (A.Y.).

References

[1] A. Yamaguchi, T. Komori, T. Suda, Regulation of osteoblast differentiation mediated by bone morphogenetic proteins, hedgehogs, and Cbfa1, Endocr. Rev. 21 (2000) 393–411.
[2] K.S. Lee, H.J. Kim, Q.L. Li, X.Z. Chi, C. Ueta, T. Komori, J.M. Wozney, E.G. Kim, J.Y. Choi, H.M. Ryoo, S.C. Bae, Runx2 is a common target of transforming growth factor beta1 and bone morphogenetic protein 2, and cooperation between Runx2 and Smad5 induces osteoblast-specific gene expression in the pluripotent mesenchymal precursor cell line C2C12, Mol. Cell. Biol. 20 (2000) 8783–8792.
[3] M.H. Lee, Y.J. Kim, H.J. Kim, H.D. Park, A.R. Kang, H.M. Kyung, J.H. Sung, J.M. Wozney, H.M. Ryoo, BMP-2-induced Runx2 expression is mediated by Dlx5, and TGF-beta 1 opposes the BMP-2-induced osteoblast differentiation by suppression of Dlx5 expression, J. Biol. Chem. 278 (2003) 34387–34394.
[4] B.K. Zehentner, C. Dony, H. Burtscher, The transcription factor Sox9 is involved in BMP-2 signaling, J. Bone Miner. Res. 14 (1999) 1734–1741.
[5] M.B. Goldring, K. Tsuchimochi, K. Ijiri, The control of chondrogenesis, J. Cell Biochem. 97 (2006) 33–44.
[6] T. Komori, H. Yagi, S. Nomura, A. Yamaguchi, K. Sasaki, K. Deguchi, Y. Shimizu, R.T. Bronson, Y.H. Gao, M. Inada, M. Sato, R. Okamoto, Y. Kitamura, S. Yoshiki, T. Kishimoto, Targeted disruption of Cbfa1 results in a complete lack of bone formation owing to maturational arrest of osteoblasts, Cell 89 (1997) 755–764.
[7] P. Ducy, R. Zhang, V. Geoffroy, A.L. Ridall, G. Karsenty, Osf2/Cbfa1: a transcriptional activator of osteoblast differentiation, Cell 89 (1997) 747–754.
[8] C.A. Yoshida, T. Furuichi, T. Fujita, R. Fukuyama, N. Kanatani, S. Kobayashi, M. Satake, K. Takada, T. Komori, Core-binding factor beta interacts with Runx2 and is required for skeletal development, Nat. Genet. 32 (2002) 633–638.
[9] H. Akiyama, Control of chondrogenesis by the transcription factor Sox9, Mod. Rheumatol. 18 (2008) 213–219.
[10] T. Liu, Y. Gao, K. Sakamoto, T. Minamizato, K. Furukawa, T. Tsukazaki, Y. Shibata, K. Bessho, T. Komori, A. Yamaguchi, BMP-2 promotes differentiation of osteoblasts and chondroblasts in Runx2-deficient cell lines, J. Cell Physiol. 211 (2007) 728–735.
[11] Y. Arimatsu, Latexin: a molecular marker for regional specification in the neocortex, Neurosci. Res. 20 (1994) 131–135.
[12] Y. Liang, G. Van Zant, Aging stem cells, latexin, and longevity, Exp. Cell. Res. 314 (2008) 1962–1972.
[13] Y. Liang, M. Jansen, B. Aronow, H. Geiger, G. Van Zant, The quantitative trait gene latexin influences the size of the hematopoietic stem cell population in mice, Nat. Genet. 39 (2007) 178–188.
[14] E. Balint, D. Lapointe, H. Drissi, C. van der Meijden, D.W. Young, A.J. van Wijnen, J.L. Stein, G.S. Stein, J.B. Lian, Phenotype discovery by gene expression profiling: mapping of biological processes linked to BMP-2-mediated osteoblast differentiation, J. Cell Biochem. 89 (2003) 401–426.
[15] T. Katagiri, A. Yamaguchi, M. Komaki, E. Abe, N. Takahashi, T. Ikeda, V. Rosen, J.M. Wozney, A. Fujisawa-Sehara, T. Suda, Bone morphogenetic protein-2 converts the differentiation pathway of C2C12 myoblasts into the osteoblast lineage, J. Cell Biol. 127 (1994) 1755–1766.
[16] Y. Uratani, K. Takiguchi-Hayashi, N. Miyasaka, M. Sato, M. Jin, Y. Arimatsu, Latexin, a carboxypeptidase A inhibitor, is expressed in rat peritoneal mast cells and is associated with granular structures distinct from secretory granules and lysosomes, Biochem. J. 346 (Pt 3) (2000) 817–826.
[17] Y. Hatanaka, Y. Uratani, K. Takiguchi-Hayashi, A. Omori, K. Sato, M. Miyamoto, Y. Arimatsu, Intracortical regionality represented by specific transcription for a novel protein, latexin, Eur. J. Neurosci. 6 (1994) 973–982.
[18] H. Akiyama, M.C. Chaboissier, J.F. Martin, A. Schedl, B. de Crombrugghe, The transcription factor Sox9 has essential roles in successive steps of the chondrocyte differentiation pathway and is required for expression of Sox5 and Sox6, Genes Dev. 16 (2002) 2813–2828.
[19] T. Furumatsu, M. Tsuda, K. Yoshida, N. Taniguchi, T. Ito, M. Hashimoto, H. Asahara, Sox9 and p300 cooperatively regulate chromatin-mediated transcription, J. Biol. Chem. 280 (2005) 35203–35208.
[20] T. Ikeda, S. Kamekura, A. Mabuchi, I. Kou, S. Seki, T. Takato, K. Nakamura, H. Kawaguchi, S. Ikegawa, U.I. Chung, The combination of SOX5, SOX6, and SOX9 (the SOX trio) provides signals sufficient for induction of permanent cartilage, Arthritis. Rheum. 50 (2004) 3561–3573.
[21] Y. Han, V. Lefebvre, L-Sox5 and Sox6 drive expression of the aggrecan gene in cartilage by securing binding of Sox9 to a far-upstream enhancer, Mol. Cell. Biol. 28 (2008) 4999–5013.
[22] A. Aagaard, P. Listwan, N. Cowieson, T. Huber, T. Ravasi, C.A. Wells, J.U. Flanagan, S. Kellie, D.A. Hume, B. Kobe, J.L. Martin, An inflammatory role for the mammalian carboxypeptidase inhibitor latexin: relationship to cystatins and the tumor suppressor TIG1, Structure 13 (2005) 309–317.
[23] E. Arikawa-Hirasawa, H. Watanabe, H. Takami, J.R. Hassell, Y. Yamada, Perlecan is essential for cartilage and cephalic development, Nat. Genet. 23 (1999) 354–358.
[24] H.P. Sørensen, R.R. Vivès, C. Manetopoulos, R. Albrechtsen, M.C. Lydolph, J. Jacobsen, J.R. Couchman, U.M. Wewer, Heparan Sulfate Regulates ADAM12 through a molecular switch mechanism, J. Biol. Chem. 283 (2008) 31920–31932.
[25] M. Kobayashi, Y. Naomoto, T. Nobuhisa, T. Okawa, M. Takaoka, Y. Shirakawa, T. Yamatsuji, J. Matsuoka, T. Mizushima, H. Matsuura, M. Nakajima, H. Nakagawa, A. Rustgi, N. Tanaka, Heparanase regulates esophageal keratinocyte differentiation through nuclear translocation and heparan sulfate cleavage, Differentiation 74 (2006) 235–243.
[26] M. Jin, M. Ishida, Y. Katoh-Fukui, R. Tsuchiya, T. Higashinakagawa, S. Ikegami, Y. Arimatsu, Reduced pain sensitivity in mice lacking latexin, An inhibitor of metallocarboxypeptidases, Brain Res. 1075 (2006) 117–121.

Biochemical and Biophysical Research Communications 381 (2009) 339–344

Contents lists available at ScienceDirect

Biochemical and Biophysical Research Communications

journal homepage: www.elsevier.com/locate/ybbrc

Early exercise in spinal cord injured rats induces allodynia through TrkB signaling

Teruaki Endo [a], Takashi Ajiki [a], Hirokazu Inoue [a], Motoshi Kikuchi [b], Takashi Yashiro [b], Sueo Nakama [a], Yuichi Hoshino [a], Takashi Murakami [c], Eiji Kobayashi [c,*]

[a] Department of Orthopedic Surgery, Jichi Medical University, Shimotsuke, Tochigi 329-0498, Japan
[b] Division of Histology, Department of Anatomy, Jichi Medical University, Shimotsuke, Tochigi 329-0498, Japan
[c] Division of Organ Replacement Research, Center for Molecular Medicine, Jichi Medical University, 3311-1 Yakushiji, Shimotsuke, Tochigi 329-0498, Japan

ARTICLE INFO

Article history:
Received 9 February 2009
Available online 15 February 2009

Keywords:
Spinal cord injury
Assisted stepping exercise
Neuronal regeneration
Neuropathic pain
Allodynia
Brain-derived neurotrophic factor
Tropomyosin-related kinase B

ABSTRACT

Rehabilitation is important for the functional recovery of patients with spinal cord injury. However, neurological events associated with rehabilitation remain unclear. Herein, we investigated neuronal regeneration and exercise following spinal cord injury, and found that assisted stepping exercise of spinal cord injured rats in the inflammatory phase causes allodynia. Sprague–Dawley rats with thoracic spinal cord contusion injury were subjected to assisted stepping exercise 7 days following injury. Exercise promoted microscopic recovery of corticospinal tract neurons, but the paw withdrawal threshold decreased and C-fibers had aberrantly sprouted, suggesting a potential cause of the allodynia. Tropomyosin-related kinase B (TrkB) receptor for brain-derived neurotrophic factor (BDNF) was expressed on aberrantly sprouted C-fibers. Blocking of BDNF–TrkB signaling markedly suppressed aberrant sprouting and decreased the paw withdrawal threshold. Thus, early rehabilitation for spinal cord injury may cause allodynia with aberrant sprouting of C-fibers through BDNF–TrkB signaling.

Introduction

Rehabilitation is commonly considered for spinal cord injured patients. In particular, rehabilitation plays a very important role in preventing muscle contraction and joint stiffness in patients with spinal cord injury [1], leading to an improvement in the quality of life of the patient. While it may be impossible for patients to perform voluntary exercise, assisted stepping exercise with partial weight bearing, referred to as "Body Weight Supported Treadmill Training (BWSTT)", has been investigated in the clinical setting [2]. Indeed, it has been demonstrated that BWSTT can improve the locomotor capacity of spinal transected rats [3]. Our previous studies also showed that assisted stepping exercise yielded beneficial effects in terms of functional recovery in hindlimb transplanted rats [4]. Nonetheless, the significance of such early rehabilitation in patients following spinal cord injury in the inflammatory phase remains unclear, and little is known about the efficiency of early rehabilitation in terms of neurological symptoms.

Herein, we focused on investigating the relationship between early exercise following spinal cord injury and neuronal regeneration, and found that early assisted stepping exercise for spinal cord injured rats promoted neuronal regeneration but caused allodynia with aberrant sprouting of C-fibers through BDNF–TrkB signaling.

Materials and methods

Rat spinal cord injury model. Adult female Sprague–Dawley (SD) rats were used. All animal experiments in this study were approved by the Animal Ethics Review Board of Jichi Medical University, and were performed in accordance with the Jichi Medical University Guide for Laboratory Animals and followed the principles of laboratory animal care formulated by the National Society for Medical Research.

Rats were anesthetized with an intraperitoneal injection of pentobarbital (40 mg/kg). Laminectomy of T9 was performed without disrupting the dura. Following laminectomy, a bilateral contusion injury was reliably created by delivering a 200 kdyn (2.00 N) force directly onto the spinal cord using an Infinite Horizon Impactor (Precision Systems and Instrumentation, MA). Following impaction, rats were maintained in a pathogen-free room under constant environmental control and subjected to twice-daily manual bladder expressions as necessary until urinary function returned.

Assisted stepping exercise for spinal cord injured rats. Spinal cord injured rats were subjected to assisted stepping exercise using the Rodent Robot 3000 (Robomedica, CA) robotic device [3]. This system consists of a motorized treadmill, a pair of robotic arms,

* Corresponding author. Fax: +81 285 44 5365.
E-mail address: eijikoba@jichi.ac.jp (E. Kobayashi).

0006-291X/$ - see front matter © 2009 Elsevier Inc. All rights reserved.
doi:10.1016/j.bbrc.2009.02.043

and a body weight support system mechanism. The rat steps bipedally in the device, and robotic arms attached to the lower shank of each hindlimb force the hindlimb to move with a normal walking pattern. A body weight support system is used to partially unload the hindlimb and stabilize the rat during stepping.

Rats were divided according to the absence or presence of exercise. The trained group ($n = 12$) was subjected to exercise, performed for 8 weeks from 1 week after the injury, 10 min per day, 5 days per week. The body weight support system supported 75% of the animal's body weight. The treadmill speed was 11 cm/s. Rats belonging to the non-trained group ($n = 11$) were not subjected to exercise.

Locomotor assessment. The functional outcomes were assessed using the Basso, Beattie, and Bresnahan Locomotor Rating Score (BBB score) for rat hindlimb motor function [5]. The assessment was performed every week until 9 weeks following the injury.

Measurement of hind paw withdrawal threshold. The hind paw withdrawal threshold was measured using the von Frey hair test [6]. Rats were placed in a plastic cage with a wire mesh bottom that allowed full access to the paws. The paw was touched with a series of von Frey hairs in ascending order beginning with the lowest hair. The hair was presented perpendicular to the planter surface with sufficient force to cause slight buckling against the paw and held there for 5 s. A withdrawal response was considered valid only if the hind paw was completely removed from the platform. The test was conducted three times using the same hair while the withdrawal response was observed. If a withdrawal response was not observed, the next largest hair in the series was applied in a similar manner. When the paw was withdrawn from a particular hair, the value of that hair in grams was regarded as the withdrawal threshold. The test was performed six times for each hind paw, and the median value of the threshold was calculated for each rat. The test was performed 5 and 9 weeks following the injury.

Histological assessment. The spinal cords were collected 9 weeks following the injury. Rats were deeply anesthetized with an intraperitoneal injection of pentobarbital and perfused intracardially using 4% paraformaldehyde in 0.1 M phosphate buffer, and fixed at 4 °C for 1 h. The spinal cords were then soaked in 20% sucrose buffer at 4 °C overnight and then in 30% sucrose buffer at 4 °C for 24 h. The spinal cords were embedded in Tissue-Tek® Optimal Cutting Temperature Compound, frozen, and then 6-μm thick axial sections were cut using a cryostat. To examine the distribution of corticospinal tract neurons at the L1 level, immunostaining using anti-Ca^{2+}/calmodulin-dependent protein kinase 2 alpha subunit (CaMK2a) antibodies (diluted 1:500, mouse monoclonal; Zymed, CA) was conducted with Alexa Fluor® 488-labeled goat anti-mouse IgG (diluted 1:200; Invitrogen, CA) as secondary antibodies. In an effort to determine whether $CaMK2a^+$ fibers represent regenerating fibers, anti-growth associated protein 43 (GAP43) antibodies (diluted 1:1000, rabbit polyclonal; Millipore, MA) were used for double immunostaining, followed by the respective use of secondary antibodies Alexa Fluor® 488-labeled goat anti-mouse IgG (diluted 1:200) and Alexa Fluor® 564-labeled goat anti-rabbit IgG (diluted 1:200; Invitrogen).

To examine the distribution of C-fibers in the dorsal horn at the T1 level, immunostaining using anti-calcitonin-gene-related peptide (CGRP) antibodies (diluted 1:2000, rabbit polyclonal; Biomol, PA) was performed, followed by the use of biotin-labeled goat anti-rabbit IgG as secondary antibodies. The Vectastain Elite ABC kit (Vector, CA) was used to visualize the reaction of horseradish peroxidase (HRP)-labeled reagents with DAB Substrate solution (Vector). To determine the relationship between $CGRP^+$ fibers and regenerating fibers, double immunostaining was performed using anti-CGRP (diluted 1:2000) and anti-GAP43 antibodies (diluted 1:10,000, mouse monoclonal; Millipore, MA), coupled with Alexa Fluor® 488-labeled goat anti-rabbit IgG (diluted 1:200; Invitrogen) and Alexa Fluor® 564-labeled goat anti-mouse IgG (diluted 1:200; Invitrogen) as secondary antibodies, respectively.

To examine expression on $GAP43^+$ fibers of the tropomyosin-related kinase B receptor (TrkB), which is a high-affinity receptor for BDNF, anti-TrkB antibodies (diluted 1:100, chicken polyclonal IgY; Promega KK, Japan) were used for the double staining with either anti-CaMK2a or anti-CGRP antibodies, followed by the respective use of secondary antibodies Alexa Fluor® 488-labeled goat anti-mouse IgG (diluted 1:200) for $CaMK2a^+$ fibers, Alexa Fluor® 488-labeled goat anti-rabbit IgG (diluted 1:200) for $CGRP^+$ fibers, and Cy3-labeled goat anti-chicken IgY (diluted 1:200; Abcam, Japan) for $TrkB^+$ fibers.

For all immunostaining procedures, sections were incubated with primary antibodies at 4 °C overnight after blocking non-specific reactions with 1.5% goat serum in phosphate-buffered saline (PBS) at room temperature for 1 h. After washing with PBS, specimens were incubated with secondary antibodies at room temperature for 1 h.

TrkB inhibitors. To functionally block BDNF, TrkB Fc chimera (R&D systems, MN) and pan Trk antagonist K252a (Biomol) were administered into the injured spinal cord of trained rats. Briefly, 1 week prior to spinal cord injury an intrathecal cannula (0.64-mm outer diameter, 0.3-mm inner diameter; Alzet, CA) was filled with PBS and inserted into the intrathecal space via the intralamina space between C1 and C2 such that the tip rested above the L1 level. Six days following spinal cord injury (1 day before commencement of the stepping exercise), osmotic minipumps (models 2002; Alzet) were filled with TrkB Fc chimera in PBS (3 μg/day, $n = 7$), K252a in 10% dimethyl sulfoxide (DMSO) in PBS (2 μg/day, $n = 7$) or PBS ($n = 7$) and connected to the cannula. Continuous intrathecal infusions and exercise were then performed for 4 weeks.

Statistical analysis. Analysis of the BBB score and hind paw withdrawal thresholds involved the use of SPSS Statistics 17.0 software (SPSS Japan Inc., Tokyo, Japan). The Mann–Whitney U test was used for *post hoc* comparisons between trained and non-trained groups. The Dunnett test was employed for *post hoc* comparisons among the three groups for the TrkB signal blocking. Differences between groups were considered significant when $p < 0.05$.

Results

Assisted stepping exercise in spinal cord injured rats promotes axonal regeneration in the corticospinal tract

Spinal cord injured rats were made to walk without weight bearing on the hindlimb before exercise. The BBB score showed a gradual improvement in every rat, and all rats of the trained group (12) and 9 of the 11 rats of the non-trained group walked with full weight bearing at 9 weeks following the injury. The score of the trained group was slightly larger than that of the non-trained group between 6 and 9 weeks following the injury (data not shown).

To determine whether exercise can potentially improve locomotor capacity, immunostaining against CaMK2a was used for assessment of the corticospinal tract fibers at the L1 level. It is well known that $CaMK2a^+$ fibers represent the descending corticospinal tract fibers in the ventral aspect of the dorsal funiculus [7]. Dense $CaMK2a^+$ fibers were distributed in the corticospinal tract of normal rats (Fig. 1Aa). $CaMK2a^+$ fibers disappeared in the corticospinal tract around 1 week following spinal cord injury (Fig. 1Ab). $CaMK2a^+$ fibers in the corticospinal tract then appeared again 9 weeks following the injury, and these were more densely distributed in the trained group (Fig. 1Ad) compared to the non-trained group

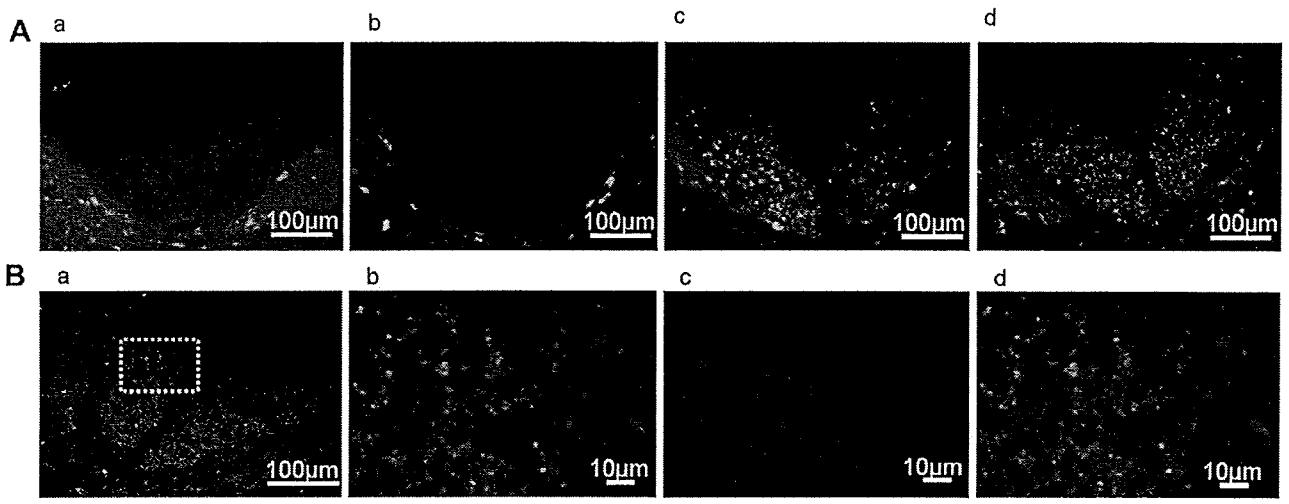

Fig. 1. Immunohistochemical assessment of the motor system of rats subjected to early rehabilitation following spinal cord contusion injury. (A) Distribution of CaMK2a$^+$ fibers in the corticospinal tract at the L1 level. In normal rats, CaMK2a$^+$ fibers were distributed in the corticospinal tract (a). CaMK2a$^+$ fibers almost disappeared at 1 week following the injury (b). CaMK2a$^+$ fibers were observed again at 9 weeks following the injury. In comparison to the non-trained group (c), CaMK2a$^+$ fibers were more densely distributed in the trained group (d). (B) Poor axonal elongation of the L1 corticospinal tract in trained rats at 9 weeks following the injury. Many CaMK2a$^+$ fibers were present in the corticospinal tract (a). High magnification of the dotted box with anti-CaMK2a (b, green) and anti-GAP43 (c, red) antibodies. CaMK2a$^+$ fibers were not merged with GAP43 $^+$ fibers (d).

(Fig. 1Ac). These results suggest that the reappearance of CaMK2a immunoactivity may be associated with regeneration of corticospinal tract neurons. Thus, to further investigate the possibility that CaMK2a$^+$ fibers represent elongated axons, immunoreactivity against GAP43 was examined because GAP43 is a well-known marker for elongated axons. The CaMK2a$^+$ fibers did not show immunoreactivity against GAP43 in the same specimens (Fig. 1Ba–d). These results demonstrated that axonal elongation in the corticospinal tract at the L1 level remained poor even after exercise. Thus, assisted stepping exercise may be associated with an increase of CaMK2a$^+$ fibers in the corticospinal tract with poor axonal elongation.

Increased axonal sprouting of C-fibers in spinal cord injured rats with assisted stepping exercise

The trained rats began to hop during the training period and avoided making contact with their hindlimbs around 4 weeks following the injury. In contrast, the non-trained rats did not avoid making such contact. These observations suggest that it became painful for trained rats to make contact with their hindlimbs. To assess the degree of pain, the hind paw withdrawal threshold was evaluated using the von Frey hair test. The mean hind paw withdrawal thresholds were 28.5 ± 4.6 g (mean ± standard error of mean) in the trained group and 60.1 ± 7.6 g in the non-trained group at 5 weeks following the injury. The threshold of the trained group was significantly smaller than that of the non-trained group ($p < 0.01$). At 9 weeks following the injury, the threshold of the trained group (21.9 ± 1.8 g) was also much smaller than that of the non-trained group (60.1 ± 7.6 g) ($p < 0.001$). These results demonstrated that assisted stepping exercise decreased the hind paw withdrawal threshold in spinal cord injured rats, suggesting that the exercise may cause neuropathic pain, especially allodynia.

The cause of allodynia in spinal cord injury may be associated with the altered distribution of C-fibers at the dorsal horn. Therefore, immunostaining against CGRP, known as a marker of C-fibers, was performed at the T1 level. Immunostaining against CGRP showed dense immunoreactivity in Rexed's lamina I and II [8,9] of the dorsal horn in all rats (Fig. 2Ba–c), in which C-fibers are known to innervate [10]. In the trained group, longitudinal CGRP fibers were present between lamina II and lamina III (Fig. 2Bc). Longitudinal CGRP$^+$ fibers were not observed in normal rats (Fig. 2Ba) or in non-trained rats (Fig. 2Bb). Immunoreactivity against GAP43 was present on longitudinal CGRP$^+$ fibers (Fig. 2C). These results demonstrated that CGRP$^+$ fibers sprouted into lamina III as a result of exercise. Thus, assisted stepping exercise may exacerbate allodynia with aberrant sprouting of C-fibers at the dorsal horn.

Implication of TrkB signaling with aberrant axonal sprouting

It has previously been shown that exercise in spinal cord injured rats restores the level of BDNF in the spinal cord [11]. In order to investigate the association between BDNF and the aberrant sprouting of C-fibers, we performed double immunostaining against CGRP and TrkB, known to be a high-affinity catalytic receptor for BDNF. Immunoreactivity of TrkB was marked on the longitudinal CGRP$^+$ fibers (Fig. 3). Therefore, aberrant sprouting of C-fibers may mediate BDNF–TrkB signaling with exercise.

Functional TrkB blocking decreased neuropathic pain associated with aberrant sprouting in spinal cord injured rats with assisted stepping exercise

To investigate a possible causal relationship between the BDNF–TrkB signaling pathway and allodynia, the von Frey hair test was performed again in the presence of TrkB inhibitors. The mean hind paw withdrawal threshold in the PBS group was significantly smaller than that of the TrkB Fc and K252a groups at 5 weeks following the injury (Fig. 4A). CGRP immunostaining also showed that longitudinal immunoreactive fibers in the dorsal horn at the T1 level were only detected in the PBS group, and not in the TrkB Fc and K252a groups (Fig. 4B). These results demonstrated that blocking of BDNF–TrkB signaling provided protection from allodynia and decreased aberrant sprouting of C-fibers in spinal cord injured rats subjected to assisted stepping exercise.

In the relevant experiments, the motor system was assessed with or without TrkB inhibitors for the trained rats. The mean BBB score showed no significant difference among these groups

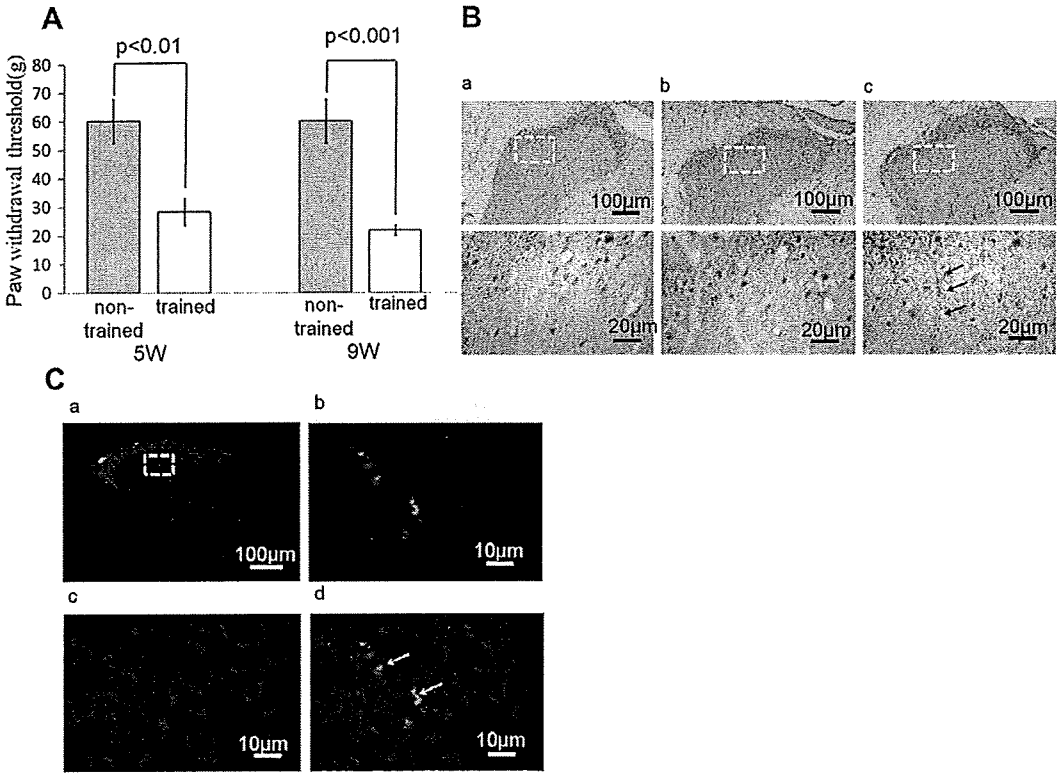

Fig. 2. Functional and immunohistochemical assessment of the sensory system of rats subjected to early rehabilitation following spinal cord contusion injury. (A) Measurement of paw withdrawal threshold using the von Frey hair test. Compared to non-trained rats, the mean paw withdrawal threshold decreased in trained rats at 5 weeks ($p < 0.01$) and 9 weeks ($p < 0.001$) following the injury. (B) Distribution of CGRP$^+$ fibers in the dorsal horn at the T1 level at 9 weeks following the injury. CGRP$^+$ fibers were distributed in lamina I and II at the dorsal horn of normal rats (a). In non-trained rats, CGRP$^+$ fibers were distributed in lamina I and II in a manner similar to that observed for normal rats (b). A longitudinal CGRP$^+$ fiber located between lamina II and III in the trained group (c). Dotted boxes in the upper panels correspond to the areas shown in the lower panels. (C) Double immunostaining against CGRP (green) and GAP43 (red) at 9 weeks following the injury in trained rats. The dotted box in panel (a) is magnified for (b–d). A longitudinal CGRP$^+$ fiber is shown between lamina II and III in the dorsal horn (a,b). Many GAP43$^+$ fibers were present in the dorsal horn (c). The longitudinal CGRP$^+$ fiber was GAP43-positive (d, arrows).

(Fig. 4C). Immunostaining against CaMK2a on the corticospinal tract at the L1 level revealed no obvious difference in the distribution of immunoreactive fibers among these groups (Fig 4D). Therefore, the motor system of spinal cord injured rats subjected to assisted stepping exercise was less affected by BDNF–TrkB signaling.

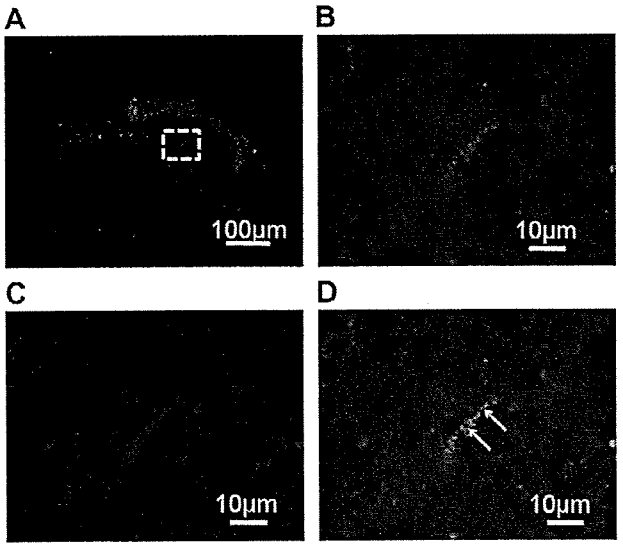

Fig. 3. TrkB expression on aberrant C-fibers in trained rats. The dotted box in (A) is magnified for (B–D). A longitudinal CGRP$^+$ fiber (green) is shown between lamina II and III (A,B). A few TrkB$^+$ fibers (red) were present in the dorsal horn (C). The longitudinal CGRP$^+$ fiber was TrkB-positive (D, arrows).

Discussion

The remarkable features presented in this study include the observations that (1) assisted stepping exercise in the inflammatory phase following spinal cord injury promoted neuronal regeneration and neuronal circuit formation, (2) the presence of allodynia was accompanied by aberrant sprouting of C-fibers, and (3) aberrant sprouting of C-fibers was mediated by BDNF-TrkB signaling.

Rehabilitation should have the potential to repair injured spinal cord as shown in previous studies [11–13]. Our studies also supported the notion that assisted stepping exercise could promote the repair of corticospinal tract neurons in spinal cord injury. However, we found that the trained rats were subject to greater pain at their hindlimbs and showed a decreased hind paw withdrawal threshold with aberrant sprouting of C-fibers compared to non-trained rats. In fact, a decreasing paw withdrawal threshold represents a major clinical finding in relation to the development of neuropathic pain, especially allodynia [6]. While it has been suggested that allodynia can develop by sprouting C-fibers to the deep layer at the dorsal horn following spinal cord injury [14], our trained rats were also subject to enhanced neuropathic pain with aberrantly sprouted C-fibers.

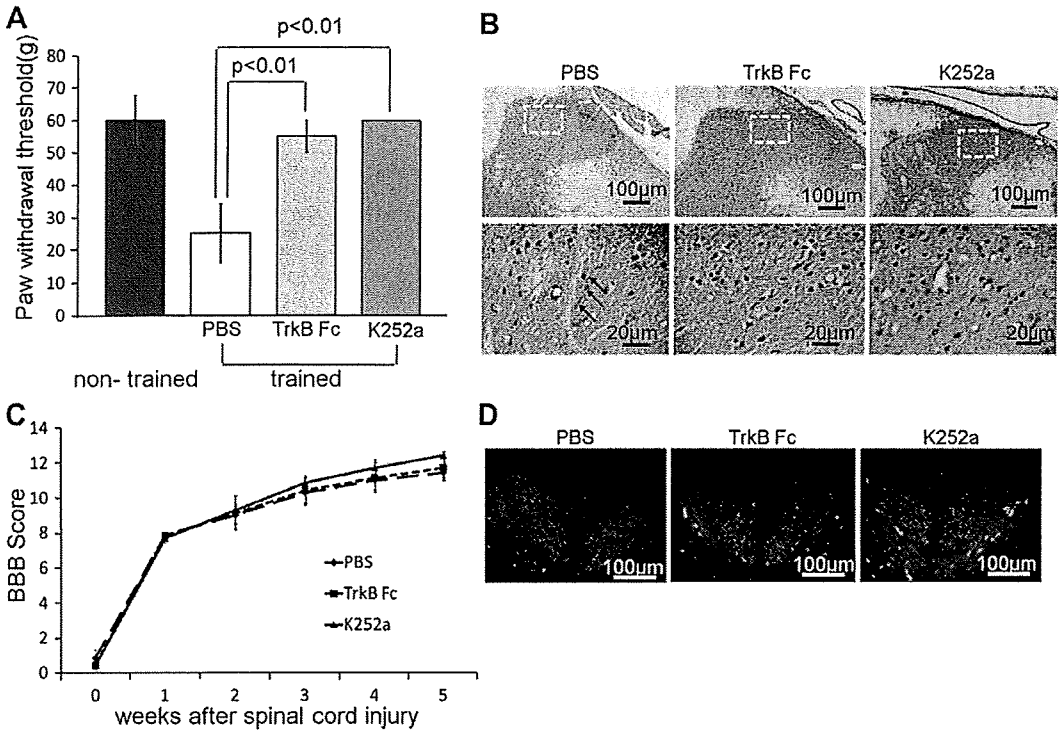

Fig. 4. Functional blocking of BDNF-TrkB signaling in trained rats. (A) Measurement of the mean paw withdrawal threshold using the von Frey hair test in the presence of TrkB-signal inhibitors. $p < 0.01$, TrkB Fc vs. PBS; $p < 0.01$, K252a vs. PBS. (B) Distribution of CGRP$^+$ fibers in the dorsal horn at the T1 level at 5 weeks following the injury. Dotted boxes in the upper column correspond to the areas shown in the lower column. A longitudinal CGRP$^+$ fiber was only observed in the PBS group, and not in the TrkB Fc and K252a groups. (C) Measurement of motor function using the BBB score. There was no significant difference in the mean BBB score among the three groups. (D) Distribution of CaMK2a$^+$ fibers in the corticospinal tract at the L1 level at 5 weeks for trained rats following the administration of TrkB inhibitors. A similar distribution of CaMK2a$^+$ fibers was observed for the three groups.

Factors that mediate the repair of an injured spinal cord with rehabilitation remain unknown. Ying et al. [11] demonstrated that voluntary exercise restored decreased levels of BDNF and increased synaptic plasticity. BDNF–TrkB signaling has been associated with axonal elongation and sprouting. Although it has been demonstrated that TrkB is expressed on A-fibers but not on C-fibers in normal rats [15], our extensive immunohistochemical findings showed that longitudinal sprouted C-fibers expressed TrkB. Therefore, increased levels of BDNF and TrkB expression on C-fibers may facilitate the sprouting of C-fibers, leading to neuropathic pain in spinal cord injured rats during early rehabilitation.

Our studies also demonstrated that aberrant sprouting of C-fibers and neuropathic pain with exercise were suppressed by the *in vivo* administration of TrkB Fc chimera or K252a. Three TrkB isoforms have been identified [16,17], and the full-length isoform (TrkB [FL]) possesses an intracellular tyrosine kinase domain that is associated with neuronal survival and differentiation [18]. In contrast, truncated isoforms (TrkB-T1 and TrkB-T2) lack tyrosine kinase activity but regulate calcium influx [17]. Since K252a can block tyrosine kinase activity, our results using blocking reagents strongly suggest that aberrant sprouting of C-fibers mediate TrkB [FL].

In conclusion, a rat early rehabilitation model following spinal cord contusion injury showed enhanced microscopic neuronal regeneration. However, subjecting injured rats to exercise also promoted aberrant sprouting of C-fibers through BDNF–TrkB signaling, leading to neuropathic pain. Thus, it is important to commence the treatment of patients with spinal cord injury so that the appropriate neural circuit can be formed without aberrant axonal sprouting. Blocking of BDNF–TrkB signaling may provide a useful adjunctive strategy in the clinical rehabilitation of patients with spinal cord injury.

Acknowledgments

We thank Dr Katsuhiko Mikoshiba (Laboratory for Developmental Neurobiology, Brain Science Institute, RIKEN, Wako, Japan) for helpful comments. This study was supported by a grant from the "Strategic Research Platform" Project for Private Universities: matching fund subsidy from MEXT (2008).

References

[1] R.M. Woolsey, Modern concepts of therapy and management of spinal cord injuries, Crit. Rev. Neurobiol. 4 (1988) 137–156.
[2] B.H. Dobkin, D. Apple, H. Barbeau, M. Basso, A. Behrman, D. Deforge, J. Ditunno, G. Dudley, R. Elashoff, L. Fugate, S. Harkema, M. Saulino, M. Scott, Methods for a randomized trial of weight-supported treadmill training versus conventional training for walking during inpatient rehabilitation after incomplete traumatic spinal cord injury, Neurorehabil. Neural Repair 17 (2003) 153–167.
[3] W.K. Timoszyk, J.A. Nessler, C. Acosta, R.R. Roy, V.R. Edgerton, D.J. Reinkensmeyer, R. de Leon, Hindlimb loading determines stepping quantity and quality following spinal cord transection, Brain Res. 1050 (2005) 180–189.
[4] T. Endo, T. Ajiki, M. Minagawa, Y. Hoshino, E. Kobayashi, Treadmill training for hindlimb transplanted rats, Microsurgery 27 (2007) 220–223.
[5] D.M. Basso, M.S. Beattie, J.C. Bresnahan, A sensitive and reliable locomotor rating scale for open field testing in rats, J. Neurotrauma 12 (1995) 1–21.
[6] S.R. Chaplan, F.W. Bach, J.W. Pogrel, J.M. Chung, T.L. Yaksh, Quantitative assessment of tactile allodynia in the rat paw, J. Neurosci. Methods 53 (1994) 55–63.
[7] T. Terashima, T. Ochiishi, T. Yamauchi, Immunohistochemical detection of calcium/calmodulin-dependent protein kinase II in the spinal cord of the rat and monkey with special reference to the corticospinal tract, J. Comp. Neurol. 340 (1994) 469–479.
[8] B. Rexed, The cytoarchitectonic organization of the spinal cord in the cat, J. Comp. Neurol. 96 (1952) 414–495.
[9] C. Molander, Q. Xu, C. Rivero-Melian, G. Grant, Cytoarchitectonic organization of the spinal cord in the rat: II. The cervical and upper thoracic cord, J. Comp. Neurol. 289 (1989) 375–385.

[10] G. Skofitsch, D.M. Jacobowitz, Calcitonin gene-related peptide: detailed immunohistochemical distribution in the central nervous system, Peptides 6 (1985) 721–745.
[11] Z. Ying, R.R. Roy, V.R. Edgerton, F. Gomez-Pinilla, Exercise restores levels of neurotrophins and synaptic plasticity following spinal cord injury, Exp. Neurol. 193 (2005) 411–419.
[12] C.A. Ghiani, Z. Ying, J. de Vellis, F. Gomez-Pinilla, Exercise decreases myelin-associated glycoprotein expression in the spinal cord and positively modulates neuronal growth, Glia 55 (2007) 966–975.
[13] Y. Berrocal, D.D. Pearse, A. Singh, C.M. Andrade, J.S. McBroom, R. Puentes, M.J. Eaton, Social and environmental enrichment improves sensory and motor recovery after severe contusive spinal cord injury in the rat, J. Neurotrauma 24 (2007) 1761–1772.
[14] A.B. Ondarza, Z. Ye, C.E. Hulsebosch, Direct evidence of primary afferent sprouting in distant segments following spinal cord injury in the rat: colocalization of GAP-43 and CGRP, Exp. Neurol. 184 (2003) 373–380.
[15] S.W. Thompson, D.L. Bennett, B.J. Kerr, E.J. Bradbury, S.B. McMahon, Brain-derived neurotrophic factor is an endogenous modulator of nociceptive responses in the spinal cord, Proc. Natl. Acad. Sci. USA 96 (1999) 7714–7718.
[16] R. Klein, D. Conway, L.F. Parada, M. Barbacid, The trkB tyrosine protein kinase gene codes for a second neurogenic receptor that lacks the catalytic kinase domain, Cell 61 (1990) 647–656.
[17] C.R. Rose, R. Blum, B. Pichler, A. Lepier, K.W. Kafitz, A. Konnerth, Truncated TrkB-T1 mediates neurotrophin-evoked calcium signalling in glia cells, Nature 426 (2003) 74–78.
[18] S.P. Squinto, T.N. Stitt, T.H. Aldrich, S. Davis, S.M. Bianco, C. Radziejewski, D.J. Glass, P. Masiakowski, M.E. Furth, D.M. Valenzuela, P.S. Distefano, G.D. Yancopoulos, TrkB encodes a functional receptor for brain-derived neurotrophic factor and neurotrophin-3 but not nerve growth factor, Cell 65 (1991) 885–893.

Biochemical and Biophysical Research Communications xxx (2009) xxx–xxx

Contents lists available at ScienceDirect

Biochemical and Biophysical Research Communications

journal homepage: www.elsevier.com/locate/ybbrc

Characterization of hepatic sexual dimorphism in Alb-DsRed2 transgenic rats

Yukitomo Arao [a], Yoji Hakamata [b], Yuka Igarashi [c], Yuki Sato [c], Fujio Kayama [a], Masafumi Takahashi [d], Eiji Kobayashi [c], Takashi Murakami [c,*]

[a] Division of Environmental Medicine, Center for Community Medicine, Jichi Medical University, Tochigi 329-0498, Japan
[b] Department of Basic Science, School of Veterinary Nursing and Technology, Faculty of Veterinary Science, Nippon Veterinary and Life Science University, Tokyo 180-8206, Japan
[c] Division of Organ Replacement Research, Center for Molecular Medicine, Jichi Medical University, 3311-1 Yakushiji, Shimotsuke, Tochigi 329-0498, Japan
[d] Division of Cardiovascular Science, Department of Organ regeneration, Shinshu University Graduate School of Medicine, Nagano 390-8621, Japan

ARTICLE INFO

Article history:
Received 29 January 2009
Available online xxxx

Keywords:
Sexual dimorphism
Pituitary hormone
Hepatocytes
Transgenic rat

ABSTRACT

We previously created the Alb-DsRed2 transgenic (Tg) rat that specifically expresses the red fluorescent protein, DsRed2, in the liver. Herein, we demonstrate that the DsRed2 expression is sexually dimorphic and exhibits a male-specific pattern. The profiling of sexual dimorphism in DsRed2 expression during pre-pubertal development was investigated using an *in vivo* fluorescent imaging analysis. The DsRed2 expression decreased gradually in both sexes until 28 days after birth. While DsRed2 expression was not persistent in the female liver, the male hepatic expression increased again at 35 days. Sexual dimorphic DsRed2 expression did not change in gonadectomized male and female Tg-rats. However, female hepatic DsRed2 was induced 72 h after the hypophysectomy. Hepatocytes isolated from the female Tg-rats also revealed DsRed2 induction by 96 h in culture. These results suggest that the pituitary hormone suppresses the female hepatic DsRed2 expression causing the sexual dimorphism of DsRed2 expression.

Introduction

Physiological differences between males and females exist in a variety of tissues, including some not usually considered sexually dimorphic. The rodent liver is one example that has provided an excellent model for investigating the complex interplay of hormonal, developmental, and tissue-specific control of gene expression [1,2]. There is a sex-specific pattern of liver gene expression for several cytochrome P450 enzymes involved in steroid and xenobiotic metabolism [3,4]. Early studies of male-specific hepatic gene expression revealed that neonatal exposure to testosterone initiated male-specific pulsatile secretion of growth hormone (GH) from the pituitary [5]. Male-specific gene expression in the adult male liver is maintained by pulsatile GH secretion [6,7]. On the other hand, adult female rats are characterized by a more frequent pituitary GH release and the near-continuous presence of GH in plasma [8]. Many studies have focused on male-specific pulsatile GH-dependent gene activation [9,10]. However, there is little information on the inactivation of male-specific genes in the female liver.

In a previous article we reported the development of the Alb-DsRed2 transgenic (Tg) rat that was designed with liver-specific expression of the red fluorescent protein, DsRed2 [11]. Interestingly, the expression of DsRed2 in this Tg animal is repressed in the female liver during pre-pubertal development, and hepatic DsRed2 is considered a male-specific protein resulting from sexually dimorphic regulation. In the current study, we focused on the regulation of hepatic DsRed2 expression in the Tg rat as a model to explore the repression mechanism of male-specific genes in the female liver. To determine the expression level of hepatic DsRed2, we employed an *in vivo* bio-imaging system based on the detection of fluorescence. The *in vivo* imaging of light-emitting probes, such as fluorescent proteins or firefly luciferase, is a powerful strategy that has enabled a wide range of biological studies to be undertaken in living animals [11–13]. Imaging reporters with light emission in the red to infrared wavelengths (>600 nm) are preferred because of the high transmission of light through tissues at these wavelengths. DsRed2, therefore, is an attractive choice for *in vivo* applications for this reason [14]. Herein, we demonstrate that hepatic DsRed2 expression levels can be evaluated quantitatively using an *in vivo* fluorescent imaging system. The use of this system revealed that pituitary hormone-mediated repression of DsRed2 in the female liver contributed to the sexually dimorphic expression of hepatic DsRed2.

Materials and methods

Experimental animals. Alb-DsRed2 transgenic male and female rats [Wistar-Tg(Alb-DsRed2)34Jmsk], which were established as

Abbreviations: GH, Growth hormone; Tg, transgenic; IVIS, *in vivo* bio-imaging system; Hypox, hypophysectomy; STAT, signal transducer and activator of transcription.

* Corresponding author. Fax: +81 285 44 5365.
E-mail address: takmu@jichi.ac.jp (T. Murakami).

0006-291X/$ - see front matter © 2009 Elsevier Inc. All rights reserved.
doi:10.1016/j.bbrc.2009.02.119

reported previously [11], were used in all experiments. To evaluate the effect of gonadal hormones and pituitary hormones on hepatic DsRed2 expression, 5-week-old male and female rats were gonadectomised and 8-week-old male and female rats were hypophysectomised, respectively. The effect of gonadectomy was investigated 3 weeks after the operation and the effect of hypophysectomy was investigated 72 h after the operation. The effectiveness of the hypophysectomy was verified by the absence of pituitaries or fragments at necropsy. All experiments in this study were performed in accordance with the Jichi Medical University Guide for Laboratory Animals.

Quantification of hepatic DsRed2 expression. The animals were anaesthetized by isoflurane and operated upon to expose the liver. DsRed2 expression levels in the liver were quantified *in vivo* using the non-invasive bio-imaging system IVIS™ (Xenogen, Alameda, CA). DsRed2 fluorescence was excited by light at 560 nm, and light emission at 600 nm from the liver tissue was collected using a cooled charge-coupled device camera [14]. Living Image software (Xenogen) was used to quantify the fluorescent signals, which were expressed as digitizing unit (photon/sec/cm^2/steradian). The expression of DsRed2 was also visualized using fluorescent microscopy under 560-nm excitation light.

Reverse Transcription-Polymerase Chain Reaction (RT-PCR). Total hepatic RNA was extracted using ISOGEN (Nippon Gene, Japan) according to the manufacturer's instructions. To eliminate genomic DNA, extracted RNA was incubated with 0.05 U/μl DNase I (Ambion) at 37 °C for 60 min. Hepatic RNA was reverse transcribed in 20-μl reaction mixes containing 1 nmol oligo dT (18mer), 400 U ReverTra Ace (Toyobo, Japan), 50 mM Tris/HCl (pH 8.3), 75 mM KCl, 3 mM $MgCl_2$, 10 U human placental RNase inhibitor (Takara, Tokyo, Japan) and 1.1 mM dNTPs, and incubated at 42 °C for 60 min [15]. PCR was performed using specific primer sets for rat CYP2C11 (upstream 5′-TAC TTT CCC TGC CAT TAT TGA TTA CTT CCC TG-3′ belonging to exon 5 of CYP2C11 and downstream 5′-ACG TGT TTC AGC AGC AGC AGG AGT C-3′ belonging to exon 6 of CYP2C11), rat CYP2C12 (upstream 5′-TTC AAC GCA TTC CCT ATT CTT CTG G-3′ belonging to exon 5 of CYP2C12 and downstream 5′-CAA AAG TGC AAA TCT CAG CGT TAA GC-3′ belonging to exon 6 of CYP2C12), and rat actin (purchased from Funakoshi, Japan). The PCR of CYP2C11 was run for 20 cycles (96 °C for 30 s, 64 °C for 50 s and 72 °C for 4 min), the PCR of CYP2C12 was run for 20 cycles (96 °C for 30 s, 59 °C for 50 s and 72 °C for 4 min), and the PCR of rat actin was run for 18 cycles (96 °C for 30 s, 60 °C for 50 s and 72 °C for 4 min) using Takara *Taq* (Takara). Aliquots (10 μl) of PCR products were resolved on 2% (w/v) agarose gels stained with ethidium bromide.

Primary culture for rat hepatocytes. Hepatocytes were prepared as previously described [16]. Briefly, hepatocytes were isolated from 10-week-old rats using a two-step collagenase perfusion method and centrifuged at 50*g* for 1 min. The cell pellet was used as a fraction of parenchymal hepatocytes. Two million hepatocytes were resuspended in 2 ml of hepatocyte culture medium (Biocoat Cell Environments, BD Biosciences, Bedford, USA) with epidermal growth factor (50 ng/ml) and then cultured. DsRed2 expression was observed using fluorescent microscopy under 560-nm excitation light.

Results

Evaluation of hepatic DsRed2 expression levels in vivo using an in vivo bio-imaging system

To investigate the regulation of hepatic DsRed2 expression, we first confirmed measurements of *in vivo* DsRed2 expression. We compared results from the *in vivo* bio-imaging system (IVIS) with those obtained from fluorescent microscopy using excitation light at 560 nm. As shown in Fig. 1A, there was a good correlation between the results obtained from each technique, and we concluded that the IVIS could accurately quantify hepatic DsRed2 expression levels *in vivo*.

Differential expression of DsRed2 in adult male and female liver

As reported previously, liver-specific DsRed2 expression observed from embryonic day 14.5 during development was maintained in newborn Tg rats [11]. Indeed, DsRed2 fluorescence was strong in newborns of both sexes, being $2.07 \times 10^8 \pm 0.65 \times 10^8$ and $3.74 \times 10^8 \pm 0.65 \times 10^8$ units (mean ± SD; $n = 4$) in male and female rats, respectively. There was no statistical difference between DsRed2 levels of male and female newborn rats. However, DsRed2 expression differed between male and female rats by the age of 5 weeks, with fluorescence levels being $2.09 \times 10^9 \pm 1.55 \times 10^9$ units (mean ± SD; $n = 4$) in male rats and $2.52 \times 10^7 \pm 0.84 \times 10^7$ units (mean ± SD; $n = 4$) in female rats. To determine when the sexual dimorphic expression of hepatic DsRed2 occurred during prepubertal development, the fluorescence level of DsRed2 in individual male and female rats was determined every 7 days after birth (Fig. 1B). The hepatic DsRed2 level increased slightly 7 days after birth in males (2.20×10^9 units) and females (1.41×10^9 units), and progressively decreased 21 days after birth in both sexes. The DsRed2 level remained undetectable in the female rat liver beyond the 28th day. In contrast, the hepatic DsRed2 level in males increased 35 days after birth (3.96×10^9 unit). Similar sex-specific profiles were observed for an additional 3 males and 1 female (data not shown).

To compare these results with the endogenous sexual dimorphic gene expression, we analyzed the hepatic mRNA levels of *CYP2C11* (male-specific) and *CYP2C12* (female-specific) in male and female Tg rats 7, 21 and 42 days after birth. As shown in Fig. 1C, expression of *CYP2C11* was not detected in female liver until day 42. In contrast, male hepatic *CYP2C11* mRNA was not detected until day 21, and increased drastically by day 42. The expression of hepatic *CYP2C12* increased in both sexes by day 21, and male hepatic *CYP2C12* expression disappeared after 42 days. These results suggested that the DsRed2 expression profile is similar to the *CYP2C11* expression profile except during the early stage of pre-pubertal development.

Female hepatic DsRed2 expression is repressed by pituitary hormone

To determine the effect of sex hormones on the sexual dimorphic expression of DsRed2 in the liver, 3 male and 3 female Tg rats were gonadectomized at 5 weeks of age (Fig. 2). The fluorescence level of hepatic DsRed2 in pre-castrated male rats was $1.13 \times 10^9 \pm 0.47 \times 10^9$ units (mean ± SD); this level was maintained ($1.21 \times 10^9 \pm 0.30 \times 10^9$ units; mean ± SD) 3 weeks after castration. On the other hand, the fluorescence level of DsRed2 in female liver was undetectable in both the pre- and post-ovariectomy (3 weeks after operation) stages. These results suggested that sex hormones do not maintain the sexual dimorphic expression of DsRed2 in adult Tg rats. We then investigated the effect of pituitary hormone on the DsRed2 expression. Three male and 3 female rats were hypophysectomized (Hypox) at 8 weeks of age, and the expression level of DsRed2 was determined before (pre-Hypox) and 72 h after (post-Hypox) the hypophysectomy. As shown in Fig. 3A, the fluorescence level of hepatic DsRed2 in pre-Hypox male rats was $8.18 \times 10^9 \pm 5.13 \times 10^9$ units (mean ± SD); this level increased by a factor of 1.3 ($1.08 \times 10^{10} \pm 0.46 \times 10^{10}$ units; mean ± SD) in post-Hypox male rat liver. The fluorescence level of hepatic DsRed2 in pre-Hypox female rats was $1.14 \times 10^8 \pm 0.87 \times 10^8$ units (mean ± SD), and increased by a factor of 36 ($4.10 \times 10^9 \pm 2.99 \times 10^9$ units; mean ± SD) in post-Hypox female

Please cite this article in press as: Y. Arao et al., Characterization of hepatic sexual dimorphism in Alb-DsRed2 transgenic rats, Biochem. Biophys. Res. Commun. (2009), doi:10.1016/j.bbrc.2009.02.119

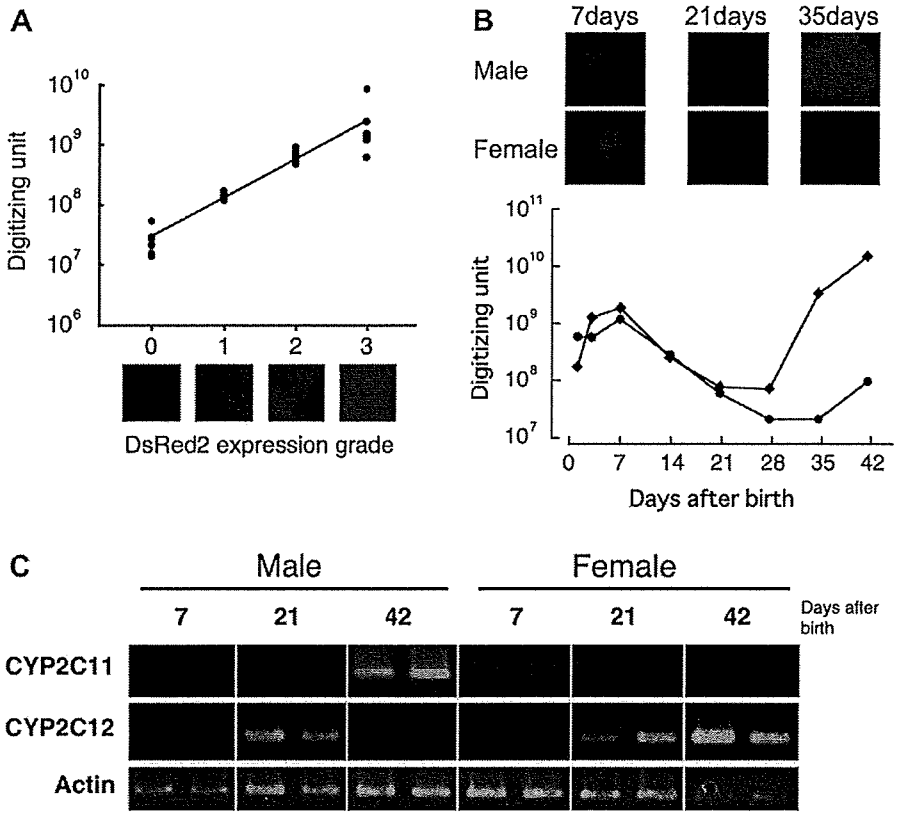

Fig. 1. DsRed2 expression in the transgenic rat liver is regulated in a sexually dimorphic manner. (A) The visible DsRed2 fluorescent signals correlate with the calculated digitizing units from the IVIS. Expressed DsRed2 was visualized by fluorescent microscopy under 560-nm excitation light. The DsRed2 expression grade was determined as indicated in the lower panel (grades 0–3; typical results are shown). Hepatic DsRed2 expression levels in the liver were detected simultaneously using the IVIS as described in Materials and methods. (B) Hepatic DsRed2 expression at 7, 21 and 35 days after birth was visualized using fluorescent microscopy (upper panels). DsRed2 expression levels in individual male (closed diamond) and female (closed circle) rat liver were detected every 7 days using the IVIS (lower panel). (C) *CYP2C11* and *CYP2C12* mRNA levels in the transgenic rat liver. Total hepatic RNA was extracted from 7-, 21- and 42-day-old transgenic animals. Reverse transcripts were amplified with a PCR technique using CYP2C11-, CYP2C12- and actin-specific primer sets as described in Materials and methods. The results obtained from two different animals are shown.

rat liver. Furthermore, we checked the expression level of hepatic *CYP2C11* and *CYP2C12* mRNAs in Hypox Tg rats (Fig. 3B). The expression level of *CYP2C12* mRNA did not change in pre- and post-Hypox female Tg rat liver. In contrast, hepatic *CYP2C11* mRNA significantly increased in post-Hypox female Tg rats that coincided with the DsRed2 expression.

DsRed2 expression in cultured Tg rat hepatocytes

Cultured hepatocytes isolated from Tg rat liver were used to evaluate the effect of circulating hormone(s) on DsRed2 repression.

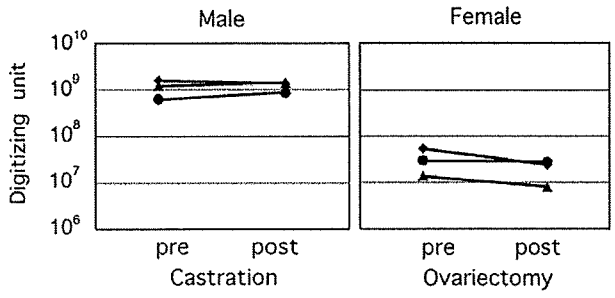

Fig. 2. Gonadal hormones have no effect on maintenance of sexual dimorphic DsRed2 expression in transgenic rat liver. Hepatic DsRed2 levels in male and female transgenic rats were detected before (pre) and 3 weeks after (post) gonadectomy. Hepatic DsRed2 levels from individual animals were detected using IVIS and the results are shown for respective animals.

As shown in Fig. 4, the expression of DsRed2 was maintained until 96 h after culture in male Tg rat hepatocytes. On the other hand, the expression of DsRed2 in female Tg rat hepatocytes was detected at 24 h following culture and increased gradually to reach a maximum at 96 h. These results support the notion that the pituitary hormone(s) in circulation represses DsRed2 expression in the female liver.

Discussion

The secretion of pituitary GH is regulated in a sexually dimorphic manner [5,8]. Adult male rats secrete GH in a highly pulsatile manner followed by GH-free intervals. In contrast, adult female rats are characterized by a more frequent pituitary GH release and the near-continuous presence of GH in plasma. The sexual differences regarding pulsatile plasma GH profile associated with adult male rats transiently induce repeated cycles of liver STAT5b activation, followed by STAT5b deactivation [17]. The continuous presence of GH in adult female rats leads to the activation of STAT5b at a low level [18]. It is thought that the status of STAT5b controls male-dominant gene expression. In this study, we demonstrated that hepatic DsRed2 levels in hypophysectomized Tg rats increased drastically in females and slightly in males (Fig. 3A). Furthermore, quiescent DsRed2 expression in female hepatocytes was activated during culture without GH (Fig. 4). These results suggest that DsRed2 expression is not activated by a GH-STAT5b pathway. The expression of DsRed2 is controlled by a mouse albumin

Please cite this article in press as: Y. Arao et al., Characterization of hepatic sexual dimorphism in Alb-DsRed2 transgenic rats, Biochem. Biophys. Res. Commun. (2009), doi:10.1016/j.bbrc.2009.02.119

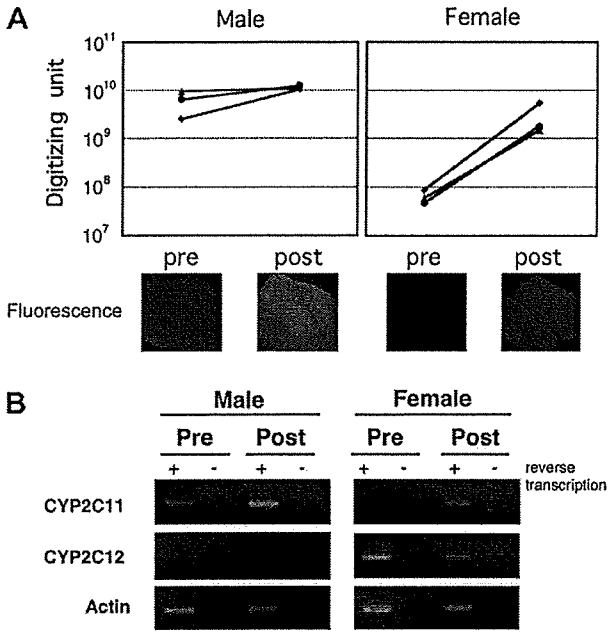

Fig. 3. Pituitary hormone represses DsRed2 expression in female transgenic rat liver. (A) Hepatic DsRed2 levels in male and female transgenic rats were detected before (pre) and 72 h after (post) hypophysectomy. Hepatic DsRed2 levels from individual animals were detected using IVIS and the results are shown for respective animals (upper panel). Hepatic DsRed2 expression was visualized using fluorescent microscopy as described Fig. 1A. A representative result is shown in the lower panel. (B) *CYP2C11* and *CYP2C12* mRNA levels in transgenic rat liver. Total RNA from hypophysectomized transgenic rat liver was reverse transcribed (RT) with (+) or without (−) reverse transcriptase. RT products were amplified with a PCR technique using CYP2C11-, CYP2C12- and actin-specific primer sets as described in Materials and methods. Representative results are shown.

promoter, which contains a −10.5 to −8.5 kb region of a 5′-flanking sequence of a mouse albumin gene and works specific in the liver [11]. We, therefore, examined the effect of a STAT5-mediated GH signal on this promoter activity using g2A-rbGHR-Jak2 cells (provided by Dr. Stuart J. Frank), and subsequently confirmed that this promoter activity was not affected by GH (data not shown). These results suggest that the repression of DsRed2 expression in the female liver is a critical factor in the sexually dimorphic expression of DsRed2.

We demonstrated that the expression of the *CYP2C11* gene, endogenous male liver-specific gene, was activated in the Hypox female rat liver similar to hepatic DsRed2 expression (Fig. 3B). The results suggest that the pituitary hormone-mediated repression of male-specific genes in the female liver may represent a general regulation of sexual dimorphic gene expression in the liver. The Alb-DsRed2 Tg rat system provides a good tool to analyze the physiological regulation of quiescent male-specific genes in female liver.

By utilizing recent advances in *in vivo* bio-imaging systems, we were able to quantify hepatic DsRed2 expression without killing experimental animals. This is an advantage if analysis is required during pre-pubertal development. For example, our data successfully suggest that 21–28 days after birth is the critical point concerning the sexual dimorphic expression of hepatic DsRed2. It is well known that neonatal exposure to testosterone produces hepatic sexual dimorphic gene expression [5]. The Alb-DsRed2 Tg animal and DsRed2 fluorescence analysis may be useful in revealing important time points regarding testosterone exposure and the effect of environmental hormones on hepatic sexual dimorphism. Furthermore, our results suggest that hepatic DsRed2 expression in Alb-DsRed2 Tg rats should be a good indicator for the physiological regulation of the hypothalamo-pituitary-liver axis in regard to adult sexual dimorphic gene expression. In fact, Liao et al. [19] demonstrated that the diethylnitrosamine (DEN)-mediated reduction of sexual dimorphism in the rat liver is partly caused by pituitary damage. It is conceivable that Alb-DsRed2 Tg animals may be useful in screening DEN-like chemicals. Thus, the Alb-DsRed2 Tg rat in couple with a novel bio-imaging system becomes a powerful tool for the study of chemicals that affect the hypothalamo-pitui-

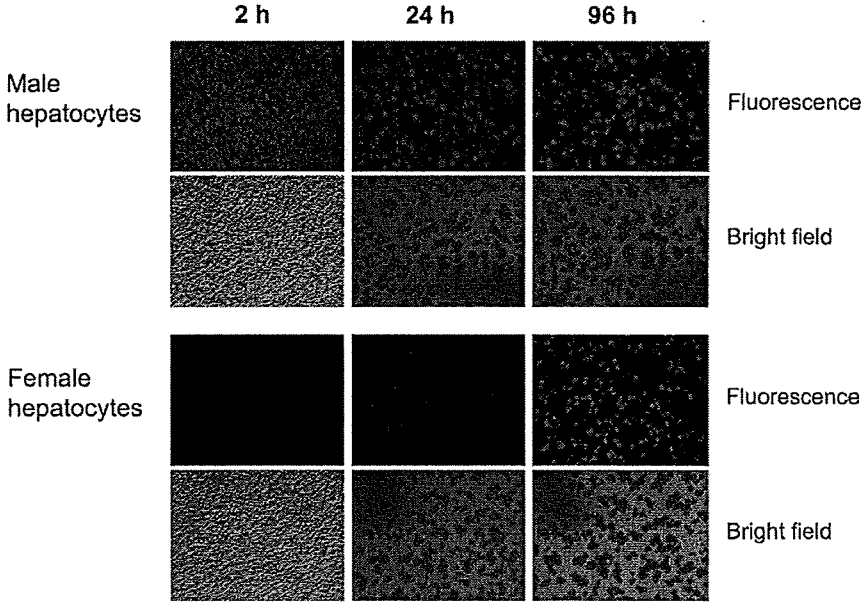

Fig. 4. DsRed2 expression in female Tg rat hepatocytes is induced during culture. Male and female hepatocytes were cultured for 96 h as described in Materials and methods. DsRed2 was detected using a fluorescent microscope under 560-nm excitation light 2, 24 and 96 h after spreading the cells (DsRed2 expressing cells are shown as Fluorescence).

Please cite this article in press as: Y. Arao et al., Characterization of hepatic sexual dimorphism in Alb-DsRed2 transgenic rats, Biochem. Biophys. Res. Commun. (2009), doi:10.1016/j.bbrc.2009.02.119

tary-liver axis in the regulation of sexual dimorphic gene expression in the neonate and adult.

Acknowledgments

We thank all personnel in the Division of Organ Replacement Research, Center for Molecular Medicine, Jichi Medical University. This study was supported by a grant from the "Strategic Research Platform" for Private Universities: matching fund subsidy from the Ministry of Education, Culture, Sports, Science and Technology of Japan. The Alb-DsRed2 Tg rat embryo is available from the Health Science Research Resources Bank (hsrrb@osa.jhsf.or.jp), National Bio-Resource Project for the Rat (nbrprat@anim.med.kyoto-u.ac.jp), or Comparative Medicine Center and Research Animal Diagnostic Laboratory, College of Veterinary Medicine, University of Missouri, MO 65211, USA (Dr. John K. Critser: critserj@missouri.edu).

References

[1] E. Lai, J.E. Darnell Jr., Transcriptional control in hepatocytes: a window on development, Trends Biochem. Sci. 16 (1991) 427–430.
[2] J.A. Gustafsson, A. Mode, G. Norstedt, P. Skett, Sex steroid induced changes in hepatic enzymes, Annu. Rev. Physiol. 45 (1983) 51–60.
[3] B.H. Shapiro, A.K. Agrawal, N.A. Pampori, Gender differences in drug metabolism regulated by growth hormone, Int. J. Biochem. Cell Biol. 27 (1995) 9–20.
[4] D.J. Waxman, Regulation of liver-specific steroid metabolizing cytochromes P450: cholesterol 7a-hydroxylase, bile acid 6ß-hydroxylase, and growth hormone-responsive steroid hormone hydroxylases, J. Ster. Biochem. Mol. Biol. 43 (1992) 1055–1072.
[5] J.O. Jansson, S. Ekberg, O. Isaksson, A. Mode, J.A. Gustafsson, Imprinting of growth hormone secretion, body growth, and hepatic steroid metabolism by neonatal testosterone, Endocrinology 117 (1985) 1881–1889.
[6] A.K. Agrawal, B.H. Shapiro, Differential expression of gender-dependent hepatic isoforms of cytochrome P-450 by pulse signals in the circulating masculine episodic growth hormone profile of the rat, J. Pharmacol. Exp. Ther. 292 (2000) 228–237.
[7] D.J. Waxman, N.A. Pampori, P.A. Ram, A.K. Agrawal, B.H. Shapiro, Interpulse interval in circulating growth hormone patterns regulates sexually dimorphic expression of hepatic cytochrome P450, Proc. Natl. Acad. Sci. USA 88 (1991) 6868–6872.
[8] A.K. Agrawal, B.H. Shapiro, Intrinsic signals in the sexually dimorphic circulating growth hormone profiles of the rat, Mol. Cell. Endocrinol. 173 (2001) 167–181.
[9] H.K. Choi, D.J. Waxman, Plasma growth hormone pulse activation of hepatic JAK-STAT5 signaling: developmental regulation and role in male-specific liver gene expression, Endocrinology 141 (2000) 3245–3255.
[10] A.S. Verma, R.N. Dhir, B.H. Shapiro, Inadequacy of the Janus kinase 2/signal transducer and activator of transcription signal transduction pathway to mediate episodic growth hormone-dependent regulation of hepatic CYP2C11, Mol. Pharmacol. 67 (2005) 891–901.
[11] Y. Sato, Y. Igarashi, Y. Hakamata, T. Murakami, T. Kaneko, M. Takahashi, N. Seo, E. Kobayashi, Establishment of Alb-DsRed2 transgenic rat for liver regeneration research, Biochem. Biophys. Res. Commun. 311 (2003) 478–481.
[12] Y. Sato, T. Ajiki, S. Inoue, J. Fujishiro, H. Yoshino, Y. Igarashi, Y. Hakamata, T. Kaneko, T. Murakami, E. Kobayashi, Gene silencing in rat-liver and limb grafts by rapid injection of small interference RNA, Transplantation 79 (2005) 240–243.
[13] Y. Hakamata, T. Murakami, E. Kobayashi, "Firefly rats" as an organ/cellular source for long-term in vivo bioluminescent imaging, Transplantation 81 (2006) 1179–1184.
[14] B.W. Rice, M.D. Cable, M.B. Nelson, In vivo imaging of light-emitting probes, J. Biomed. Opt. 6 (2001) 432–440.
[15] Y. Arao, A. Kikuchi, M. Kishida, M. Yonekura, A. Inoue, S. Yasuda, S. Wada, K. Ikeda, F. Kayama, Stability of A+U-rich element binding factor 1 (AUF1)-binding messenger ribonucleic acid correlates with the subcellular relocalization of AUF1 in the rat uterus upon estrogen treatment, Mol. Endocrinol. 18 (2004) 2255–2267.
[16] C. Tateno, K. Takai-Kajihara, C. Yamasaki, H. Sato, K. Yoshizato, Heterogeneity of growth potential of adult rat hepatocytes in vitro, Hepatology 31 (2000) 65–74.
[17] D.J. Waxman, P.A. Ram, S.H. Park, H.K. Choi, Intermittent plasma growth hormone triggers tyrosine phosphorylation and nuclear translocation of a liver-expressed, Stat 5-related DNA binding protein. Proposed role as an intracellular regulator of male-specific liver gene transcription, J. Biol. Chem. 270 (1995) 13262–13270.
[18] H.K. Choi, D.J. Waxman, Growth hormone, but not prolactin, maintains, low-level activation of STAT5a and STAT5b in female rat liver, Endocrinology 140 (1999) 5126–5135.
[19] D.J. Liao, A. Blanck, P. Eneroth, J.A. Gustafsson, I.P. Hallstrom, Diethylnitrosamine causes pituitary damage, disturbs hormone levels, and reduces sexual dimorphism of certain liver functions in the rat, Environ. Health Perspect. 109 (2001) 943–947.

Please cite this article in press as: Y. Arao et al., Characterization of hepatic sexual dimorphism in Alb-DsRed2 transgenic rats, Biochem. Biophys. Res. Commun. (2009), doi:10.1016/j.bbrc.2009.02.119

Journal of Biomedical Optics 14(5), 054017 (September/October 2009)

Profile of new green fluorescent protein transgenic Jinhua pigs as an imaging source

Tatsuo Kawarasaki
Shizuoka Prefectural Livestock Institute
Swine and Poultry Research Center
2780 Nishikata
Kikugawa, Shizuoka 439-0037, Japan

Kazuhiko Uchiyama
Kitasato University School of Medicine
Department of Laboratory Animal Science
Sagamihara, Kanagawa 228-8555, Japan

Atsushi Hirao
Jichi Medical University
Division of Anatomy
Department of Anatomy
Tochigi 329-0498, Japan

Sadahiro Azuma
Kitasato University School of Medicine
Department of Laboratory Animal Science
Sagamihara, Kanagawa 228-8555, Japan

Masayoshi Otake
Masatoshi Shibata
Seiko Tsuchiya
Shizuoka Prefectural Livestock Institute
Swine and Poultry Research Center
2780 Nishikata
Kikugawa, Shizuoka 439-0037, Japan

Shin Enosawa
National Research Institute for Child Health and Development
Department of Innovative Surgery
Tokyo 157-8535, Japan

Koichi Takeuchi
Jichi Medical University
Division of Anatomy
Department of Anatomy
Tochigi 329-0498, Japan

Kenjiro Konno
Yoji Hakamata
Jichi Medical University
Center for Experimental Medicine
Tochigi 329-0498, Japan

Hiroyuki Yoshino
Takuya Wakai
Jichi Medical University
Center for Molecular Medicine
Division of Organ Replacement Research
3311-1 Yakushiji
Shimotsuke, Tochigi 329-0498
Tochigi, 329-0498, Japan

Shigeo Ookawara
Jichi Medical University
Division of Anatomy
Department of Anatomy
Tochigi 329-0498, Japan

Hozumi Tanaka
Jichi Medical University
Center for Experimental Medicine
Tochigi 329-0498, Japan

Eiji Kobayashi
Takashi Murakami
Jichi Medical University
Center for Molecular Medicine
Division of Organ Replacement Research
3311-1 Yakushiji
Shimotsuke, Tochigi 329-0498, Japan

Address all correspondence to: Tatsuo Kawarasaki, D.V.M., PhD (for GFP-cloned Jinhua pigs) Swine and Poultry Research Center, Shizuoka Prefectural Livestock Institute, 2780 Nishikata, Kikugawa, Shizuoka 439-0037, Japan. Tel: 81-537-35-2291; Fax: 81-537-35-2294; E-mail: kawarasaki@sp-exp.pref.shizuoka.jp; or Takashi Murakami, M.D., PhD (for imaging), Division of Bioimaging Sciences, Center for Molecular Medicine, Jichi Medical University, 3311-1 Yakushiji, Shimotsuke, Tochigi 329-0498, Japan. Tel: 81-285-58-7446; Fax: 81-285-44-5365; E-mail: takmu@jichi.ac.jp

Abstract. Animal imaging sources have become an indispensable material for biological sciences. Specifically, gene-encoded biological probes serve as stable and high-performance tools to visualize cellular fate in living animals. We use a somatic cell cloning technique to create new green fluorescent protein (GFP)-expressing Jinhua pigs with a miniature body size, and characterized the expression profile in various tissues/organs and *ex vivo* culture conditions. The born GFP-transgenic pig demonstrate an organ/tissue-dependent expression pattern. Strong GFP expression is observed in the skeletal muscle, pancreas, heart, and kidney. Regarding cellular levels, bone-marrow-derived mesenchymal stromal cells, hepatocytes, and islet cells of the pancreas also show sufficient expression with the unique pattern. Moreover, the cloned pigs demonstrate normal growth and fertility, and the introduced GFP gene is stably transmitted to pigs in subsequent generations. The new GFP-expressing Jinhua pigs may be used as new cellular/tissue light resources for biological imaging in preclinical research fields such as tissue engineering, experimental regenerative medicine, and transplantation. [DOI: 10.1117/1.3241985]

Keywords: Jinhua pigs; green fluorescent protein; biological probes; somatic cell cloning.

Paper 08411RR received Nov. 20, 2008; revised manuscript received Jul. 26, 2009; accepted for publication Jul. 28, 2009; published online Oct. 12, 2009.

1 Introduction

Imaging has become an indispensable tool in both the biological sciences and medicine. In the past two decades, there has been a huge increase in the number of imaging technologies and their applications. In particular, fluorescent imaging has been most rapidly adapted for *in vitro* and *in vivo* analysis of biological processes.[1] Visualization of processes occurring in

1083-3668/2009/14(5)/054017/9/$25.00 © 2009 SPIE

the complex environment of the cell and/or tissue needs an appropriate cellular marking procedure, and fluorescent dye has often been used as a straightforward technique. However, since fluorescent intensity may decrease during *in vivo* cellular proliferation, the use of fluorescent dye is not always suitable for *in vivo* imaging.[2] Therefore, genetically encoded biological probes serve as stable and high-performance tools to visualize cellular fate in living animals.

The development of genetic molecular tags such as green fluorescent protein (GFP) from the jellyfish (*Aequorea victoria*) has mostly accelerated the revolution occurring in this field over the past decade. In fact, GFP as the most popular biological light source has offered important opportunities for the investigation of a wide variety of biological processes in living cells and animals.[3,4] To obtain a stable optic cellular source, we developed GFP-transgenic (Tg) animals, including rats and rabbits.[2,5] These GFP-Tg animals have been employed as valuable cellular and organ sources for cell therapy and transplantation studies.[6–9] For instance, the cultured stem/progenitor cells of GFP-Tg rats transplanted into the spinal cord survived for a long time after transplantation (around 50 days), demonstrating a stable *in vivo* GFP expression.[6] Moreover, application to oligodendrocyte replacement in models of white matter insult and disease also demonstrated the engraftment and survival of GFP-positive oligodendrocytes in the host white matter and cerebral cortex.[9] Thus, the evidence suggests that GFP-Tg animals provide stable cell sources even after cell proliferation and differentiation.

Recent advances in gene manipulation allowed the development of a variety of transgenic animals,[10–12] and the procedure used for the microinjection of animal zygotes has continuously improved.[13,14] However, since expression of an injected expression vector depends on the integration site of the genome and the copy number, it is not always easy to obtain transgenics that ubiquitously express a particular cDNA, even under the general promoter.[15] In fact, our previous results demonstrated that the tissue/organ expression profile depended on the line of established Tg animals.[2] Nonetheless, the characteristics of established Tg animals led to high-demand animal resources for new biomedical translational research fields such as tissue engineering and regeneration medicine. Since the use of authentic transgenic technology through microinjection into zygotes is not always suitable with large transgenic animals, we aimed to generate cloned pigs on the basis of the somatic cell nuclear transfer method[16,17] and the supportive method for reconstructed embryos.[18] In this study we generate new GFP-Tg Jinhua pigs, determine the expression profile of GFP emission light in the Tg pig, and demonstrate a stable reproductive performance. The GFP Tg pig may represent a valuable large-animal resource.

2 Experimental Materials and Methods

2.1 *Plasmid Construction and Polymerase Chain Reaction*

The pEGFPneo expression vector [Fig. 1(a)] was generated by insertion of the PGKneo polyA cassette from the pGKNeoPolyA/pUC19 plasmid into the pCX-GFP vector. The expression plasmids, pCX-GFP and pGKNeo poly-A, were kindly provided by Kashiwazaki (University of Tsukuba, Tsukuba, Japan). GFP cDNA was driven under the chicken β-actin promoter and cytomegalovirus immediate-early 1 gene enhancer.[19] The liner HindIII fragment of the pEGFPneo expression plasmid was transferred into primary fibroblasts of Jinhua pigs (see next).

For confirmation of GFP transduction into the cloned pig, polymerase chain reaction (PCR) was performed using AmpliTaq Gold polymerase (Applied Biosystems Incorporated, Foster City, California). The EGFP sequence was amplified using the following primers: forward, 5′-TGA ACC GCA TCG AGC TGA AGG G-3′; reverse, 5′-TCC AGC AGG ACC ATG TGA TCG C-3′. PCR conditions for each set of primers included initial treatment at 94°C for 2 min, followed by 35 cycles consisting of denaturation at 94°C for 30 sec, annealing at 65°C for 30 sec, followed by extension at 72°C for 2 min. PCR products (307 bp) were analyzed on a 1.5% agarose gel.

2.2 *Animals and Preparation of Transgenic Donor Cells*

Chinese Jinhua pigs were maintained under an experimental protocol approved by the Judging Committee of Transgenic Experiments of Shizuoka Prefectural Swine and Poultry Research Center and Experimental Animal Ethics of Jichi Medical University. Primary fibroblasts from the skin of a 4-day-old female Jinhua pig were grown to confluency in a 100-mm tissue culture dish. Cells (10^6 to 10^7) were trypsinized and transduced with the liner pEGFPneo (10 μg) using an electroporation system [Gene Pulser II; Bio-Rad Company, Limited, Hercules, California; at 0.240 kV, 500 μF in 900 μl of phosphate buffered saline (PBS) without Ca^{2+} and Mg^{2+}]. Electroporated cells were then cultured in a 100-mm-diam culture dish and maintained with Dulbecco modified Eagle medium (DMEM) (11965-092; Gibco, Carlsbad, California) containing 10% fetal bovine serum (FBS) and 150 μg/ml G418 geneticin (Gibco) at 37°C in a humidified atmosphere of 5% CO_2 in air for 2 weeks. The cells were trypsinized and moved onto 48-well culture plates with one cell per well. GFP-expressing cells were cultured until confluency in 35-mm-diam culture dishes, and thereafter in 60-mm dishes over the course of 6 months. The cells were frozen before nuclear transfer. Donor cells for nuclear transfer were cultured until confluency in a 35-mm dish and produced a synchronized cell cycle by serum starvation (0.5% FBS-DMEM) for 6 days.

2.3 *Somatic Cell Nuclear Transfer*

Mature oocytes and parthenogenotes were produced by methods previously described.[18] Immature oocytes of ovaries collected from a local abattoir were cultured for 40 h, and the maturity of the oocytes was assessed under a stereoscopic microscope. Only oocytes that possessed a distinct first polar body were classified as reaching metaphase 2 and used for nuclear transfer. Nuclear transfer was performed using the microinjection method.[16,17] The nuclei were each introduced into a single enucleated oocyte by piezo-actuated microinjection. Electrostimulation was performed 48 h after the start of maturation (2 to 4 h after nucleus microinjection) in an activation medium containing 280-mM D-mannitol, 0.05-mM $CaCl_2$, 0.1-mM $MgSO_4$, and 0.01% (w/v) polyvinyl alcohol. Pulses were delivered to cells placed between two wire elec-

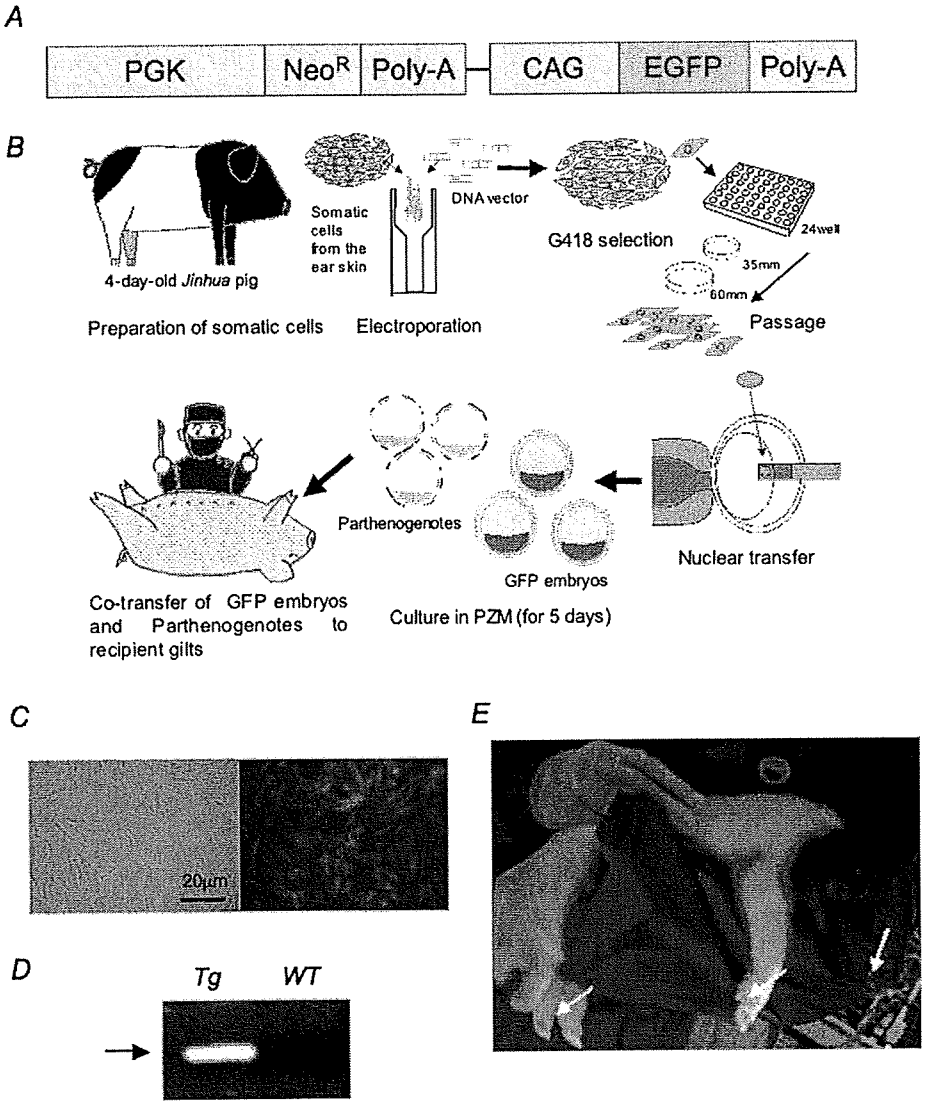

Fig. 1 Establishment of GFP-expressing Jinhua pigs. Representative scheme of the transgene composition. (a) The neomycin-resistant gene (Neo^R) is driven under a mouse phosphoglycerate kinase 1 promoter (PGK), and the enhanced GFP cDNA is driven under the chicken β-actin promoter and cytomegalovirus immediate-early 1 gene enhancer (CAG).[19] (b) Representative scheme of the creation of a cloned pig. (c) GFP expression in cells for nuclear transfer. A G418-resistant single fibroblast was grown in culture. Left panel, visible light; right panel, excitation light. Original magnification 100×. (d) Genotype inspection of a cloned pig. GFP-specific sequences were detected by PCR analysis. Tg, transgenic pig; WT, wild-type pig. (e) Representative image of the generated cloned pig under an excitation light. Arrows indicate parts with strong GFP expression (skin, oral and nasal mucosa, hoof wall).

trodes (1 mm apart) in a fusion dish (CUY5000P1, Nepa Gene Company, Limited, Ichikawa, Japan) by applying a single direct-current pulse of 150 kV/cm for a duration of 99 μsec. The stimulated oocytes were transferred to porcine zygote medium (PZM)[20] supplemented with cytochalasin B (4 μg/ml) for 2 h to prevent cytokinesis, after which the culture was continued in PZM containing 0.3% bovine serum albumin at 38.5°C under 5% O_2 and 5% CO_2 for 110 h. After this period, reconstructed embryos that developed into morula-blastocysts were transferred to the uteri of surrogate sows with parthenogenetic embryos developed at the same stage.[18]

2.4 *Isolation and Culture of Mesenchymal Stromal Cells In Vitro Differentiation Assay, and Hepatocyte Isolation*

Bone marrow cells (BMCs) from cloned pigs were harvested by flushing femurs with ice-cold PBS. Cells were filtered through a 70-μm nylon mesh and plated in T75-cm^2 or T225-cm^2 flasks with DMEM/F-12 (Gibco, Grand Island,